The essential role of a ubiquitin ligase, Riplet, in RIG-I-dependent antiviral innate immune responses

[1,3]Hiroyuki Oshiumi, [1]Moeko Miyashita [2]Naokazu Inoue, [2]Masaru Okabe, [1]Misako Matsumoto, and [1]Tsukasa Seya

[1]Department of Microbiology and Immunology, Graduate School of Medicine, Hokkaido University, Kita-15, Nishi-7, Kita-ku Sapporo 060-8638, Japan
[2]Research Institute for Microbial Diseases, Osaka University, 3-1 Yamadaoka, Suita, Osaka 565-0871, Japan

Running title: Riplet is essential for RIG-I-mediated signaling

[3]To whom correspondence should be addressed: Department of Microbiology and Immunology, Graduate School of Medicine, Hokkaido University, Kita-15, Nishi-7, Kita-ku, Sapporo 060-8638, Japan
Tel.: 81-11-706-5056; Fax: 81-11-706-7866
E-mail: oshiumi@med.hokudai.ac.jp

Summary

RIG-I plays an important role in antiviral response by recognizing intracellular viral RNA and is regulated by Lys63-linked polyubiquitination. TRIM25 ubiquitin ligase polyubiquitinates RIG-I, and is essential for RIG-I activation. Another ubiquitin ligase, Riplet, also mediates polyubiquitination of RIG-I; however, its importance remains to be determined. To examine the importance of Riplet in RIG-I-dependent innate immune response, we generated Riplet knockout mice. Interestingly, our genetical analysis showed that Riplet is essential for the production of type I interferons and other cytokines by fibroblasts, macrophages, and conventional dendritic cells during viral infection. Furthermore, the knockout of Riplet abolished RIG-I activation during viral infection, and Riplet knockout mice were more susceptible to viral infection than wild-type mice. Taken together, our data indicate that Riplet-mediated polyubiquitination of RIG-I is essential for innate immune response against viral infection in vivo.

Highlights

Cytoplasmic viral RNA sensor, RIG-I, requires Riplet for its activation.

Knockout of Riplet abolishes type I interferon production during viral infection.

Riplet is essential for protection against viral infection in vivo.

Introduction

RNA virus infection is initially recognized by RIG-I-like receptors, RIG-I and MDA5, which induce antiviral responses such as the production of type I interferons (IFNs) and proinflammatory cytokines (Yoneyama and Fujita, 2009; Takeuchi and Akira, 2010). Analyses of RIG-I and MDA5 knockout mice showed that RIG-I is essential for type I IFN production by mouse embryonic fibroblasts (MEFs), conventional dendritic cells (cDCs), and macrophages (Mf) in response to RNA viruses such as VSV, influenza A virus (Flu), hepatitis C virus (HCV) Sendai virus (SeV), and Japanese encephalitis virus (JEV). MDA5 is critical in picornavirus infection (Kato et al., 2006; Saito et al., 2007). However, in plasmacytoid DCs (pDCs), loss of RIG-I has no effect on viral induction of IFNs, and TLR7 and MyD88 are required for inducing immune responses in these cells (Diebold et al., 2004; Kato et al., 2005; Kumar et al., 2006; Sun et al., 2006).

RIG-I consists of two N-terminal CARDs, a central DExD/H helicase domain, and a C-terminal repressor domain (CTD) (Yoneyama et al., 2004). Before viral infection, CTD of RIG-I suppresses N-terminal CARDs (Saito et al., 2007). When the CTD of RIG-I recognizes the 5' triphosphate-double-stranded (ds) viral RNA, the conformation of the RIG-I protein changes, and the N-terminal CARD triggers interaction with its downstream partner IPS-1 (Hornung et al., 2006; Pichlmair et al., 2006; Saito et al., 2007; Cui et al., 2008; Takahasi et al., 2008; Rehwinkel et al., 2010). IPS-1 contains an N-terminal CARD that interacts with the tandem CARDs of RIG-I and a C-terminal transmembrane domain that localizes it to the mitochondrial outer membrane (Kawai et al., 2005; Meylan et al., 2005; Seth et al., 2005; Xu et al., 2005). IPS-1 activates TBK1 kinase, which mediates phosphorylation of IRF-3, leading to its dimerization and translocation into the nucleus (Kumar et al., 2006; Sun et al., 2006). The IRF-3 dimers, NF-κB, and AP-1 transcription factors activate type I IFN transcription (Honda et al., 2005). The secreted type I IFNs activates the IFNAR, which leads to phosphorylation and nuclear translocation of STAT1 (Akira et al., 2006; Honda et al., 2006).

RIG-I is regulated by ubiquitination. Three E3 ubiquitin ligases, RNF125; TRIM25; and Riplet, target RIG-I (Arimoto et al., 2007; Gack et al., 2007; Oshiumi et al., 2009). RNF125 functions as a negative regulator for RIG-I signaling and mediates Lys48-linked polyubiquitination of RIG-I, leading to protein degradation by the proteasome (Arimoto et al., 2007). On the other hand, TRIM25 and Riplet function as positive regulators for the signaling. TRIM25 mediates Lys63-linked polyubiquitination at Lys-172 of RIG-I CARDs (Gack et al., 2007). Lys63-linked polyubiquitination induces interaction between RIG-I and IPS-1 CARDs, leading to the activation of signaling (Gack et al., 2007; Gack et al., 2008). However, there are several reports that describe other models. Firstly, Zeng et al. developed

an in vitro reconstitution system of the RIG-I pathway (Zeng et al., 2010). Using this system, they showed that Lys-172 of RIG-I CARDs is required for binding to the Lys63-linked polyubiquitin chain (Zeng et al., 2010). They postulated that polyubiquitin binding and not ubiquitin modification is required for RIG-I activation (Zeng et al., 2010). In their model, unanchored polyubiquitin chains are responsible for RIG-I activation. However, they did not rule out the possibility that ubiquitination of some signaling proteins may contribute to RIG-I activation (Zeng et al., 2010). Secondly, Fujita T and his colleagues reported that residue-172 of mouse RIG-I is not Lys but Gln and human RIG-I K172R mutant was normally activated by SeV infection in RIG-I KO MEFs (Shigemoto et al., 2009).

The third ubiquitin ligase, Riplet, mediates Lys63-linked polyubiquitination of RIG-I CTD and CARDs (Gao et al., 2009; Oshiumi et al., 2009). This polyubiquitination promotes RIG-I activation and its antiviral activity in human cells (Horner and Gale, 2009; Nakhaei et al., 2009; Takeuchi and Akira, 2010; Yoneyama and Fujita, 2010); however, in vivo evidence is absent. Type I IFNs are mainly produced by DCs or Mf in vivo, and RIG-I is essential for type I IFNs production in cDC and Mf (Kato et al., 2005; Sun et al., 2006; Kumagai et al., 2007). The role of Riplet in these cells also has not yet been examined. Both TRIM25 and Riplet proteins mediate Lys63-linked polyubiquitination of RIG-I, and thus Gao et al. suggested that Riplet may be a complementary factor of TRIM25 for RIG-I activation (Gao et al., 2009). Therefore, it is not known whether Riplet is essential for RIG-I activation. To address these issues, we generated Riplet knockout mice. Our analysis revealed that Riplet is essential for the RIG-I activation and innate immune responses against viral infection in vivo. This is the first report to show that a ubiquitin ligase targeting RIG-I is essential for an antiviral response in vivo.

Results

Ubiquitous Expression of Riplet mRNA

Firstly, we examined mouse Riplet mRNA expression by quantitative PCR (qPCR), and found it to be ubiquitously expressed in various tissues, MEFs, bone marrow-derived DCs (BM-DCs), and Mf (BM-Mf) (Figure 1A left panel). Furthermore, we have previously shown that human Riplet mRNA is expressed in various tissues. When we examined the expression of Riplet mRNA in human DCs, it was observed in human DCs as in HeLa cells (Figure 1A right panel). These data indicate that Riplet is expressed in various tissues and cells that are able to produce type I IFNs.

Generation of Riplet-Deficient Mice

Previously, we have shown that Riplet is a positive regulator for RIG-I-mediated signaling, and it mediates Lys63-linked polyubiquitination of the C-terminal region of RIG-I. However, the functional role of Riplet in vivo remains unclear. To investigate the role of Riplet in vivo, we generated Riplet-deficient (Riplet −/−) mice by homologous recombination of ES cells (Figure 1B). We confirmed the target disruption of Riplet without deletion outside the targeted region (Figure 1C and Figure S1). Riplet mRNA expression was abolished in Riplet −/− cells (Figure 1E and 1F), and the knockout of Riplet did not affect the expression of other genes, such as RIG-I, MDA5, IPS-1, TICAM-1, TLR3, and TRIM25, which are involved in type I IFN production (Figure 1F). The mutant mice were born at the Mendelian ratio from Riplet +/− parents (Figure 1D), and they developed and bred normally. These mice displayed no apparent abnormalities up to 7 months of age. Mutations in the human Riplet/RNF135 gene cause the overgrowth syndrome (Douglas et al., 2007). We did not observe any overgrowth phenotypes in Riplet +/− and Riplet −/− mice. Next, we examined the composition of CD4-, CD8-, CD11c-, and/or PDCA1-positive cells in the spleen, and found no difference between wild-type and Riplet −/− mice (Figure S2). Induction of cDC from BM in the presence of GM-CSF was also normal in Riplet −/− mice (Figure S2). Therefore, the mouse Riplet gene is dispensable for development.

Riplet −/− Embryonic Fibroblasts Are Defective in Innate Immune Responses Against RNA Viruses

Riplet is a positive regulator for RIG-I mediated signaling. In mouse fibroblast, VSV and Flu are mainly recognized by RIG-I (Kato et al., 2006). Furthermore HCV 3’ UTR RNA is also recognized by RIG-I (Saito et al., 2008). Therefore, we first examined the expression of type I IFNs, IFN-inducible gene IP-10, and Ccl5 in MEFs after HCV 3’ UTR dsRNA

transfection or infection with VSV or Flu. The induction of mRNA of IFN-α2, -β, IP-10, and Ccl5 in response to VSV or Flu was abrogated in Riplet −/− MEFs (Figure 2A-2D). In addition, transfection of low concentration of HCV 3' UTR dsRNA (0.05-0.2 μg/well) also failed to upregulate IFN-α2, -β, and IFN-inducible genes in Riplet −/− MEFs (Figure 2A-2D).

Single-stranded (ss) RNA, which is synthesized by T7 RNA polymerase in vitro, induced lower IFN-β expression than dsRNA (Figure S3A). The induction of IFN-β mRNA by HCV 3' UTR ssRNA was also abolished in Riplet −/− MEFs (Figure S3A). Although the induction of IFN-β mRNA in response to VSV infection was abrogated in Riplet −/− MEFs even at high (MOI = 5) or low multiplicities of infection (MOI = 0.2 or 1), the induction of IFN-β mRNA in response to high concentration of HCV dsRNA (0.8 μg/well) was detected in Riplet −/− MEFs (Figure S4A-S4C). Therefore, RIG-I does not require Riplet function in the presence of large amounts of naked viral RNA in the cytoplasmic region.

Recently, Onoguchi et al. reported that type III IFN, IFN-λ, induction was RIG-I dependent during viral infection (Onoguchi et al., 2007). The induction of IFN-λ mRNA in response to VSV was also abrogated in Riplet −/− MEFs (Figure S3B).

Next, we examined type I IFNs or IL-6 levels in culture supernatants after viral infection or HCV 3' UTR RNA transfection (low concentration condition). The production of IFN-α, -β, and IL-6 in culture supernatants was abrogated in Riplet −/− MEFs (Figure 3A-3C). Next, we analyzed the contribution of Riplet to the antiviral response. When MEFs were infected with VSV at various MOI, cytopathic effects (CPEs) were more severe in Riplet −/− than wild-type MEFs (Figure 3D). These results demonstrate that Riplet plays a critical role in the elimination of RNA virus infection by induction of IFN responses.

Riplet is Dispensable for the Production of Type I IFN Induced by B-DNA and HSV-1 Infection

Cytoplasmic B-form double-stranded DNA (dsDNA) stimulates the cells to induce type I IFNs and IFN-inducible genes (Ishii et al., 2006). TBK1 is required for type I IFN induction by dsDNA (Ishii et al., 2008). Although immortalized MEFs require RIG-I for type I IFNs production by dsDNA stimulation, primary MEFs do not require IPS-1, which is a RIG-I adaptor, for type I IFNs production by dsDNA (Kumar et al., 2006; Chiu et al., 2009). We examined the expression of IFN-β and IP-10 mRNA by dsDNA stimulation in primary wild-type and Riplet −/− MEFs. IFN-β and IP-10 mRNA were detected in Riplet −/− MEFs by dsDNA transfection similar to that detected in wild-type MEFs (Figure 4A and 4B).

Next, we examined IFN-β mRNA expression during infection with DNA virus, HSV-1. Wild-type and Riplet −/− MEFs were infected with HSV-1, and IFN-β mRNA expression was examined by RT-qPCR. IFN-β expression in Riplet −/− MEFs was comparable to that in wild-type MEFs (Figure 4C). Taken together, these data indicate that Riplet-dependent RIG-I activation is dispensable for type I IFN and IFN-inducible genes mRNA expression by cytoplasmic DNA in primary MEFs. This is consistent with previous studies reporting that the IPS-1-dependent pathway is dispensable for type I IFN production by cytoplasmic dsDNA stimulation (Kumar et al., 2006).

Riplet is Essential for Triggering the RIG-I Signaling Pathway

We further examined the role of Riplet in RIG-I-mediated signaling during RNA virus infection. In RIG-I-mediated signaling, induction of type I IFNs and proinflammatory cytokines requires the activation of transcription factor IRF3. IRF3 is phosphorylated by TBK1 and IKK-ε. Phosphorylated IRF3 induces IFN-β gene expression. IFN-β produced subsequently stimulates the JAK-STAT pathway to amplify the responses. To determine the role of Riplet in signaling pathway activation, we analyzed IRF3 and STAT1 activations after VSV infection in Riplet −/− MEFs. VSV-induced dimerization of IRF3 and VSV- or Flu-induced pohsphorylation of STAT1 were abrogated in Riplet −/− MEFs (Figure 3E and 3F). These results demonstrate that Riplet is essential for activating the transcription factors that work early phase of RNA virus infection.

In the absence of viral infection, RIG-I CTD suppressed N-terminal CARDs (Saito et al., 2007). After viral infection, RIG-I CTD binds to viral RNA, leading to conformational changes (Saito et al., 2007). Later, RIG-I CARDs undergo TRIM25-mediated polyubiquitination and associate with IPS-1 CARD (Gack et al., 2007; Gack et al., 2008). When we tested the effect of Riplet on RIG-I activation, the full-length RIG-I protein with CTD failed to activate the IFN-β promoter in Riplet −/− MEFs (Figure 5A); however, promoter activation by the expression of RIG-I CARDs without CTD was normal in Riplet −/− MEFs (Figure 5B). These data indicate that Riplet is required for the activation of full-length RIG-I but not for the activation of RIG-I CARDs without CTD. Next, we performed complementation assays. Immortalized Riplet −/− MEFs were transfected with an empty-, RIG-I-, or RIG-I-5KA mutant-expressing vector together with or without Riplet-expressing vector. The RIG-I-5KA mutant harbors mutations in five C-terminal Lys residues that are important for Riplet-mediated ubiquitination (Oshiumi et al., 2009). In the Riplet −/− cell line, RIG-I was not activated by HCV RNA stimulation, and Riplet expression led to the activation of wild-type RIG-I (Figure 5C). The deletion of the Riplet RING-finger domain, which is the catalytic domain of ubiquitin ligase, abolished RIG-I

activation (Figure 5D). Unlike wild-type RIG-I, Riplet expression failed to activate the RIG-I-5KA mutant protein (Figure 5C). The activations of wild-type and mutant RIG-I were correlated with its polyubiquitination (Figure S5A). Although the RNA binding activity was weakly reduced by the 5KA mutation, the pull down assay showed that RIG-I-5KA mutant bound to dsRNA (Figure S5B). Next, we examined ligand-independent RIG-I activation by overexpression of Riplet. Overexpression of Riplet in HEK293 cells activated RIG-I in the absence of RIG-I ligand, such as viral RNA (Figure S5C). This ligand-independent activation of RIG-I by Riplet overexpression was abolished by the 5KA mutation (Figure S5C). Thus, the 5KA mutation disrupts ligand-independent RIG-I activation by overexpression of Riplet. Next, we examined the polyubiquitination of exogenously expressed RIG-I CTD fragment. Polyubiquitination of RIG-I CTD fragment was increased by overexpression of Riplet (Figure S5D), and was reduced by overexpression of dominant negative form of Riplet (Riplet DN) (Figure S5E). Polyubiquitination of RIG-I CTD fragment was not detected in Riplet-deficient cell (R3T cell), however expression of Riplet caused polyubiquitination of RIG-I CTD fragment (Figure S5F). These data are consistent with our previous report (Oshiumi et al., 2009). Taken together, these data indicate that Riplet-dependent polyubiquitination of RIG-I is important for RIG-I activation.

Previously, we showed that Riplet is not involved in MDA5-mediated signaling. IFN-β promoter activation by MDA5 overexpression was normal in Riplet −/− MEFs (Figure 5E). Transfection of polyI:C, which is recognized by MDA5, induced IFN-β, IL-6, and IP-10 expression in both wild-type and Riplet −/− MEFs (Figure 5F-5H). In addition, stimulation with lipopolysaccharide (LPS), which is a TLR4 ligand, normally induced expression of these cytokines in Riplet −/− MEFs (Figure 5I-5K). Furthermore, IL-6 production in culture medium in response to LPS was normal in Riplet −/− MEFs (Figure 5L). Taken together, these data indicate that Riplet is essential for the RIG-I-mediated type I IFN or IL-6 production upon viral infection in nonprofessional immune cells like fibroblasts, but is not required for MDA5- or TLR4-mediated signaling.

Riplet is Required for Antiviral Innate Immune Responses in Conventional Dendritic Cells and Macrophages

We examined whether Riplet is required for the induction of type I IFN in DCs or Mf. DCs play a pivotal role in bridging innate and adaptive immune responses, and can be classified into cDCs and pDCs, the latter producing high levels of type I IFNs. Mf also produce type I IFN. We induced cDCs from BM cells in the presence of GM-CSF (BM-DC). Twenty-four hours after VSV or Flu infection, cDCs of wild-type mice produced IFN-α, -β, and IL-6

(Figure 6A-6F). In contrast, the cDCs of Riplet −/− mice showed severely impaired IFN-α, -β or IL-6 production during VSV or Flu infection (Figure 6A-6F). When the cDCs were stimulated with a TLR4 ligand, such as LPS, IFN-β or IL-6 production in Riplet −/− cDCs was almost normal (Figure S6A and S6B), indicating that Riplet is dispensable for LPS-induced cytokine production in cDCs.

Then, we tested M-CSF-induced BM-Mf. Wild-type Mf produced IFN-α, -β and IL-6 after VSV or Flu infection (Figure 6A-6F). Similar to cDCs, cytokine production was reduced in Riplet knockout mice (Figure 6A-6F). Peritoneal Mf were isolated from wild-type and Riplet −/− mice. Knockout of Riplet reduced type I IFN production from peritoneal Mf during VSV infection (Figure S7).

We next generated Flt3L-induced DCs (Flt3L-DCs), which contain pDCs. Akira and his colleagues previously showed that the knockout of RIG-I or IPS-1 does not reduce type I IFN and IL-6 production by Flt3L-DCs, because RIG-I is dispensable for cytokine production in pDCs (Kato et al., 2005). The Flt3L-DCs of Riplet −/− mice produced normal amounts of IFN-a, -β and IL-6 during Flu infection (Figure 6A-6F). This is consistent with the notion that Riplet is essential for the RIG-I mediated type I IFNs and IL-6 production. Although the IFN-α levels in the culture medium after VSV infection were comparable with those in wild-type and Riplet −/− mice, Flt3L-DCs of Riplet −/− mice produced less IL-6 compared with that produced by wild-type mice through an unknown mechanism (Figure 6C).

Next, we examined type I IFN production during SeV infection. SeV infection induced IFN-α and -β productions from wild-type BM-DC, and the knockout of Riplet reduced IFN-α and -β productions from BM-DC (Figure S8). Wild-type Flt3L-DC produced IFN-α after SeV infection, and the knockout of Riplet did not reduce IFN- α production from Flt3L-DC (Figure S8).

Riplet is Essential for Antiviral Immune Defense In Vivo

To investigate the role of Riplet in antiviral responses in vivo, wild-type and Riplet −/− mice were injected intraperitoneally with wild-type VSV, and sera were collected to measure type I IFN and IL-6 levels. IFN-α, –β, and IL-6 levels in sera were markedly reduced in Riplet −/− mice compared to in wild-type mice (Figure 7A and 7B and Figure S9). Next, wild-type and Riplet −/− mice were intranasally infected with VSV, and type I IFN levels in their sera were measured. At early time points, IFN-α and -β production was reduced in Riplet −/− mice compared to wild-type mice (Figure 7C and 7D); however, cytokine levels were comparable at later time points (Figure S10A and S10B). Previously, Ishikawa et al. observed that the knockout of STING gene, which is involved in

RIG-I-dependent signaling, leads to reduction of type I IFN at early time points and relatively less reduction at later time points (Ishikawa and Barber, 2008; Ishikawa et al., 2009).

To determine if Riplet deficiency affects the survival of mice after VSV infection, the mice were intranasally infected with VSV and their survival was monitored. Wild-type mice survived VSV infection; however Riplet −/− mice were susceptible to VSV infection (Figure 7E). The viral titer in Riplet −/− mice brains 7 days after infection was higher than in wild-type mice (Figure 7F). These data indicate that Riplet plays a key role in the host defenses against VSV infection in vivo, and type I IFN production at early time points is important for host defenses.

Discussion

In this study, we presented genetic evidence that Riplet is indispensable for antiviral responses in MEFs, BM-Mf, and BM-DCs, but not in Flt3L-DCs. The cell-type specific requirement of Riplet is similar to that of RIG-I. Previously, we showed that Riplet binds to RIG-I and mediates Lys63-linked polyubiquitination of RIG-I (Oshiumi et al., 2009). Genetic evidence in this study revealed that Riplet function is essential for RIG-I-dependent type I IFN production. Knockout of Riplet reduced type I IFN production in vivo during the early phase of VSV infection and Riplet −/− mice were susceptible to VSV infection. Taken together, our results provide genetic evidence that Riplet is essential for RIG-I-dependent antiviral immune response *in vivo*. Most of RIG-I −/− embryos were lethal at embryonic days 12.5 to 14.0 in some strain backgrounds (Kato et al., 2005). However, we could not observe any developmental defect in Riplet knockout mice as far as we examined.

Previously, Chen and his colleagues independently isolated Riplet and named it REUL (Gao et al., 2009). They reported that REUL/Riplet binds to RIG-I CARDs but not to CTD (Gao et al., 2009). Furthermore, they reported that REUL/Riplet mediates Lys63-linked polyubiquitination of Lys-172 of RIG-I CARDs in a manner similar to TRIM25 (Gack et al., 2007; Gao et al., 2009). Although they did not show any expression profile data for Riplet and TRIM25, they mentioned that TRIM25 and Riplet have different distribution patterns, and thus hypothesized that REUL/Riplet is a complementary factor of TRIM25 and is required for RIG-I activation in cells that do not express TRIM25 (Gao et al., 2009). However, our genetic evidence is not consistent with their hypothesis because Riplet is essential for RIG-I activation in MEFs that express TRIM25. Previously, Gack et al. showed that knockout of TRIM25 alone abolished RIG-I activation in MEFs (Gack et al., 2007). Therefore, null mutation in either Riplet or TRIM25 abolishes RIG-I activation.

These genetic evidence indicate that Riplet can mediate polyubiquitination of RIG-I Lys residues that are not ubiquitinated by TRIM25. This means that Riplet functions differently than TRIM25 in RIG-I activation.

Previously, we isolated Riplet cDNA by yeast two-hybrid screening using the C-terminal region of RIG-I (Oshiumi et al., 2009). Because the yeast genome does not encode RIG-I, the interaction indicates the direct binding of Riplet to the RIG-I C-terminal region. The interaction between RIG-I CTD and Riplet has also been confirmed by immunoprecipitation assays in human cells (Oshiumi et al., 2009). Moreover we have shown that Riplet expression leads to Lys63-linked polyubiquitination of RIG-I CTD (Oshiumi et al., 2009). Recently, Zheng et al showed that RIG-I CARDs has the ability to bind to polyubiquitin chains (Zeng et al., 2010). We have carefully detected Riplet-mediated polyubiquitination of RIG-I C-terminal region without CARDs, under high salt conditions, in which many protein-protein interactions were abolished (Oshiumi et al., 2009). Therefore, we proposed the hypothesis that Riplet mediates Lys63-linked polyubiquitination of RIG-I CTD (Oshiumi et al., 2009). This model can explain the genetic evidence that Riplet is essential for RIG-I activation in MEFs that express TRIM25. Gack et al. showed that K172R mutation alone caused near-complete loss of ubiquitination of the human RIG-I CARDs (Gack et al., 2007). Because residue-172 of mouse RIG-I is not Lys but Gln (Shigemoto et al., 2009), Riplet/Reul cannot ubiquitinate residue-172 of mouse RIG-I. Based on the previous studies and our current data, we prefer the interpretation that Riplet activates RIG-I through polyubiquitination of RIG-I CTD. However, this interpretation does not exclude the possibility that Riplet ubiquitinates both CTD and CARDs of RIG-I (Gao et al., 2009; Oshiumi et al., 2009). Previously, we showed that Lys-849, -851, -888, -907, and -909 are critical residues in Riplet-mediated RIG-I CTD ubiquitination (Oshiumi et al., 2009). These five Lys residuse are close to the dsRNA-binding sites of RIG-I CTD (Takahasi et al., 2008). It is also possible that the 5KA mutation affects on the structure or functions of RIG-I. Therefore, we do not exclude the possibility that the other Lys residues of RIG-I or other unknown factors are ubiquitinated by Riplet. Further in vitro studies are required to determine the polyubiquitination sites and to reveal precise RIG-I regulatory mechanisms by Riplet-mediated Lys63-linked polyubiquitation.

In general, E3 ubiquitin ligase targets several types of proteins. Therefore, it is possible that Riplet targets other proteins. Previous work has shown that Riplet binds to the Trk-fused gene (TFG) protein (Suzuki et al., 2001). The TFG protein interacts with TANK and NEMO, which are involved in the NF-κB pathway (Miranda et al., 2006). Although NEMO is involved in IPS-1-mediated signaling, RIG-I CARDs- or MDA5-mediated

signaling was normal in Riplet −/− MEFs. Therefore, interaction between Riplet and TFG protein is not required for RIG-I-mediated signaling. However, since TFG is involved in tumorigenesis (Miranda et al., 2006), Riplet may be involved in human tumorigenesis.

Several viral proteins inhibit RIG-I-mediated signaling. For example, Flu NS1 inhibits TRIM25 and HCV NS3/4A cleaves IPS-1 (Meylan et al., 2005; Gack et al., 2009). Therefore, Riplet may be inhibited by viral proteins. Indeed, our pilot study indicated that the Riplet protein is disrupted in human hepatocyte cell lines carrying a full-length HCV replicon. RIG-I is involved in innate immune responses against various viruses. In this study, we showed that Riplet is required for innate immune responses against VSV, Flu, and SeV. Therefore, Riplet is also expected to be involved in innate immune responses against other viruses that are recognized by RIG-I.

Experimental Procedures

Generation of Riplet-Deficient Mice

The Riplet gene was amplified by PCR using genomic DNA extracted from ES cells by PCR. The targeting vector was constructed by replacing the second and third exons with a neomycine-resistance gene cassette (Neo), and a herpes simplex virus thymidine kinase (HSV-TK) driven by PGK promoter was inserted into the genomic fragment for negative selection. After the targeting vector was transfected into 129/Sv mice-derived ES cells, G418 and gancyclovir doubly resistant colonies were selected and screened by PCR. The targeted cell line was injected in C57BL/6 blastocysts, resulting in the birth of male chimeric mice. These mice were then crossed with 129/Sv mice to obtain heterozygous mutants. The heterozygous mutants were intercrossed to obtain homozygous Riplet −/− mice.

Cells, Viruses, and Reagents

Wild-type and Riplet −/− MEFs were prepared from day 12.5-13.5-day embryos. Riplet −/− MEFs were immortalized with large T antigen and named R3T cell line. BM cells were prepared from 5- to 10-week-old mice. VSV Indiana strain was provided by A. Takada (Hokkaido University). VSV was amplified using Vero cells and the viral titer was determined by the plaque assay. Flu (PR8 strain) and SeV (HVJ strain) was provided by Y. Sakoda (Hokkaido University). HSV-1 strain was provided by K. Kondo (The JIKEI University). Anti-mouse IRF3 antibody was purchased from Zymed. Anti-phospho-STAT1 antibody was purchased from Cell Signaling and anti-STAT1 antibody from Santa Cruz. Salomon sperm dsDNA was purchased from Invitrogen. To determine the viral titer in the brain, the mice were sacrificed, and the brain was aseptically removed and the frozen at -80 ^{o}C. The brain was homogenized in 1 ml of PBS on ice, and the titer was determined by plaque assay.

Preparation of Viral Double-Stranded RNA

cDNA of the HCV 3' UTR region was amplified from total RNA of the HCV genotype 1b full-length replicon using primers HCV-F1 and HCV-R1, and then cloned in the pGEM-T Easy Vector. The primer set sequences were HCV-F1: CTC CAG GTG AGA TCA ATA GG and HCV-R1: CGT GAC TAG GGC TAA GAT GG. RNA was synthesized using T7 and SP6 RNA polymerases. Template DNA was digested by DNase I, and RNA was purified using TRIZOL (Invitrogen) according to manufacturer's instructions.

Quantitative PCR

For qPCR, total RNA was extracted with TRIZOL (Invitrogen) and 0.5 μg of RNA was reverse-transcribed using the High Capacity cDNA Transcription Kit (ABI) with random primers according to the manufacturer's instructions. qPCR was performed using the Step One Real-Time PCR system (ABI). Primer sequences used for qPCR are listed in Supplementary Table 1.

Measurement of Cytokines

In brief, 5 x 10^5 cells in a 24-well plate were either infected with VSV or Flu, stimulated with LPS, or transfected with HCV 3' UTR dsRNA or polyI:C. Twenty-four hours after infection, stimulation, or transfection, culture supernatants were collected and analyzed for IFN-α, -β, and IL-6 production by ELISA. Cytokine levels were measured in mouse serum obtained from the mouse tail vein. ELISA kits for mouse IFN-α and -β were purchased from PBL Biomedical Laboratories. ELSA kit for mouse IL-6 was purchased from Invitrogen.

Preparation of Dendritic Cells and Macrophages

BM cells were prepared from the femur and tibia. The cells were cultured in RPMI1640 medium supplemented with 10% of FCS, 100 μM of 2-Me, and 100 ng/ml of human Flt3 ligand (Pepro Tech), and 10 ng/ml of murine GM-CSF or culture supernatant of NIH3T3 expressing M-CSF. After 6 days, cells were collected and used as Flt3L-DC, GM-DC, or BM-Mf. In case of GM-DC or BM-Mf, the medium was changed every 2 days.

Native PAGE analysis

Approximately 1 x 10^6 MEFs were infected with VSV at MOI = 1 for 9 h and then lysed. Cell lysates in native PAGE sample buffer (62.5 mM Tris-HCl [pH 6.8], 15% glycerol, and BPB) were separated using native PAGE and then immunoblotted with anti-murine IRF3 antibody (Zymed).

Luciferase Assay

Expression plasmids for mouse RIG-I N-terminal CARDs, full-length RIG-I, or full-length MDA5 were constructed in pEF-BOS. The cDNA fragment encoding the ORF of RIG-I or MDA5 was amplified by RT-PCR using total RNA prepared from MEFs. The Riplet dRING mutant protein lacks 1 - 69 aa region. Wild-type and mutant (Riplet dRING) Riplet-expression vectors were described previously (Oshiumi et al., 2009). Wild-type or Riplet −/− MEFs were transiently transfected in 24-well plates with reporter constructs containing the IFN-β promoter and Renilla luciferase (internal control) together with the

empty vector (control), RIG-I CARDs, full-length RIG-I, or MDA5 expression vectors. Twenty-four hours after transfection, cells were lysed and subjected to the luciferase assay using the Dual-Luciferase Reporter Assay system (Promega).

Statistical Analyses

Statistical significance of differences between groups was determined by the Student's *t* test, and survival curves were analyzed by the logrank test using Prism 4 for Macintosh software (GraphPad Sofware, Inc.). Chi-square goodness-of-fit tests and Student's *t* tests were performed using MS-Excel software and a chi-square distribution table.

Acknowledgment

We thank Dr John P. Atkinson (Washington Univ.) and Dr. Ralph Steinman (Rockefeller Univ.) for critical discussions, Yoko Esaki and Kiyo Kawata for technical support in generating Riplet KO mice, N. Irie for a pilot study of B-DNA stimulation assay, and Sakoda Y. for technical instructions for the experiments using Flu and SeV. This work was supported in part by the Mitsubishi Foundation, Mochida Foundation, Akiyama Life Science Foundation, Grants-in-Aid from Ministry of Education, Science, and Culture and Ministry of Health, Labor, and Welfare of Japan. The authors have no conflicting financial interests.

Figure Legends

Figure 1. Targeted Disruption of the Murine Riplet Gene

(A) Riplet mRNA expression in mouse tissues and cells or human cells. RT-qPCR was performed to measure Riplet mRNA and each sample was normalized to β-actin (mouse) or GAPDH (human). Data are shown as means ± SD and are representative of three independent experiments.

(B) Structure of the mouse Riplet gene, targeting vector, and disrupted gene. Closed boxes indicate the coding exon of Riplet and hatched boxes indicate the Neo or TK gene coding region. The primer sets for PCR are shown by arrows.

(C) PCR of mouse tail. Genomic DNA was extracted from wild-type, Riplet +/−, or Riplet −/− mice tails and PCR was performed using primers shown in (B).

(D) Genotype analyses of offspring from heterozygote intercrosses. Chi-square goodness-of-fit test indicated that deviation from Mendelian ratio was not statistically significant ($P > 0.1$).

(E) RT-PCR of MEFs. Total RNA from wild-type and Riplet −/− MEFs were extracted and subjected to RT-PCR to determine Riplet mRNA expression.

(F) Riplet, IPS-1 MDA5, RIG-I, TICAM-1, TLR3, and TRIM25 expression in MEFs. Total RNA from wild-type and Riplet −/− MEFs were extracted and subjected to RT-qPCR to determine mRNA expression. Expression of the indicated gene mRNA was normalized to β-actin mRNA expression. Data are shown as means ± SD and are representative of three independent experiments. “NS” indicates no statistically significant difference between the two samples.

Figure 2. Abolished Responses to RNA Virus Infection in Riplet −/− Fibroblasts

Wild-type or Riplet −/− MEFs were infected with VSV or Influenza A virus (Flu), and total RNA was extracted at the indicated times. Short HCV 3’ UTR dsRNA was transfected into wild-type or Riplet −/− MEFs and total RNA was extracted after 24 hours. Extracted RNA was subjected to RT-qPCR to determine IFN-β (A), IP10 (B), Ccl5 (C), or IFN-α2 (D) expression. Expression of each sample was normalized to β-actin mRNA expression. Data are shown as means ± SD and are representative of three independent experiments. *$P < 0.05$, **$P < 0.01$ (*t* test)

Figure 3. Role of Riplet in Antiviral Responses in Fibroblasts

(A-C) Wild-type or Riplet −/− MEFs were infected with VSV or Flu or transfected with short HCV 3’UTR dsRNA. Amount of IFN-α (A), -β (B), and IL-6 (C) in culture supernatants were measured by ELISA after 24 h. Data are shown as means ± SD and are

representative of three independent experiments. *P < 0.05, **P < 0.01 (*t* test)
(D) Wild-type or Riplet −/− MEFs were infected with VSV at the indicated MOI, and after 36 h, MEFs were fixed with formaldehyde and stained with crystal violet.
(E) Wild-type or Riplet −/− MEFs were infected with VSV at MOI = 5, and after 9 h cell lysates were prepared and analyzed by native PAGE. IRF-3 proteins were stained with anti-IRF3 antibody.
(F) Wild-type or Riplet −/− MEFs were infected with VSV or Flu at MOI = 1, and after 20 h, cell lysates were prepared. The samples were analyzed by SDS-PAGE and Western blotting. They were stained with anti-STAT1, phospho-STAT1, or β-actin antibodies.

Figure 4. Role of Riplet in type I IFN production induced by cytoplasmic dsDNA
(A, B) Wild-type and Riplet −/− MEFs were transfected with the indicated amounts of dsDNA (Salomon sperm DNA) using the Lipofectamine 2000 reagent. Nine hours after the transfection, IFN-β (A) and IP-10 (B) mRNA expression was determined by RT-qPCR.
(C) Wild-type and Riplet −/− MEFs were infected with HSV-1 at MOI = 4, and IFN-β mRNA expression at the indicated times were examined by RT-qPCR.

Figure 5. Role of Riplet in the RIG-I-dependent pathway
(A) Expression vector of full-length RIG-I and reporter plasmids were transfected into wild-type or Riplet −/− MEFs with or without HCV 3' UTR short dsRNA, and after 24 hours, IFN-β promoter activation was examined by reporter gene assay. Data are shown as means ± SD and are representative of three independent experiments. *P < 0.05 (*t* test).
(B) Expression vector for the two RIG-I N-terminal CARDs were transfected into wild-type or Riplet −/− MEFs together with reporter plasmids, and IFN-β promoter activation was examined by the reporter gene assay. Data are shown as means ± SD and are representative of three independent experiments. "NS" indicates not statistically significant.
(C) Empty-, wild-type RIG-I-, or RIG-I-5KA mutant-expressing vectors were transfected into the Riplet −/− MEF cell line together with or without the Riplet-expressing vector. Cells were stimulated with HCV 3' UTR short dsRNA and reporter gene assay was performed as described in (A).
(D) Empty or wild-type RIG-I-expressing vectors were transfected into the Riplet −/− MEF cell line together with empty, wild-type Riplet, or Riplet mutant (Riplet dRING) -expressing vector. Cells were stimulated with HCV 3' UTR short dsRNA and the reporter gene assay was performed as described in (A).
(E) Empty or MDA5-expressing vectors was transfected into wild-type or Riplet −/− MEFs together with reporter plasmids, and after 24 h, IFN-β promoter activation was examined

by the reporter gene assay.
(F-H) 0.8 μg of polyI:C were transfected into wild-type or Riplet −/− MEFs. Twenty-four hours after transfection, total RNA was extracted from MEFs and subjected to RT-qPCR to determine IFN-β (F), Ccl5 (G), and IP10 (H) expression. Expression in each samples was normalized to the β-actin mRNA expression.
(I-K) Wild-type or Riplet −/− MEFs were stimulated with 1 μg of LPS. Total RNA was extracted at the indicated times and subjected to RT-qPCR analysis for of IFN-β (I), IL-6 (J), or IP-10 (K) expression.
(L) Wild-type or Riplet −/− MEFs were stimulated with LPS, and after 24 h the amount of IL-6 in culture supernatants was measured by ELISA.

Figure 6. Role of Riplet in Responses to VSV or Flu infection in Bone-Marrow Derived Cells
GM-DCs, BM-Mf, or Flt3L-DCs were induced from BM-derived cells in the presence of GM-CSF, M-CSF, or Flt3L and infected with VSV or Influenza A virus at MOI = 1. Twenty-four hours after viral infection, amounts of IFN-β (A, D), -α (B, E), and IL-6 (C, F) in culture supernatants were measured by ELISA. Data are shown as means ± SD and are representative of two independent experiments. *P < 0.05 (Student's *t* test). NS indicates not statistically significant.

Figure 7. Role of Riplet in Antiviral Responses In Vivo
(A, B) Wild-type or Riplet −/− mice were injected intraperitoneally with 1 x 10^6 pfu of VSV. Amounts of IFN-α (A) and IL-6 (B) in mouse serum were measured by ELISA. Data are shown as mean ± SD of samples obtained from three wild-type and three Riplet −/− mice at each time points. *P < 0.05 (Student's *t* test). "ND" indicates not detected.
(C, D) Wild-type and Riplet −/− mice were infected intranasally with 4 x 10^5 pfu of VSV. Amounts of IFN-α (C) and IFN-β (D) in mouse serum were measured by ELISA.
(E) Wild-type and Riplet −/− mice were infected intranasally with 2 x 10^6 pfu of VSV and mice mortality was observed for 14 days (*P < 0.05 between wild-type and Riplet −/− mice, logrank test).
(F) Wild-type and Riplet −/− mice were infected intranasally with 2 x 10^6 pfu of VSV, and sacrificed for their tissues on day 7 after infection. Titers in brain were determined by the plaque assay. Viral titers in brains of wild-type mice were below 100 pfu/g, and thus not detected (ND). Data are shown as means ± SD (N = 3).

References

Akira, S., Uematsu, S., and Takeuchi, O. (2006). Pathogen recognition and innate immunity. Cell *124*, 783-801.

Arimoto, K., Takahashi, H., Hishiki, T., Konishi, H., Fujita, T., and Shimotohno, K. (2007). Negative regulation of the RIG-I signaling by the ubiquitin ligase RNF125. Proc Natl Acad Sci U S A *104*, 7500-7505.

Chiu, Y.H., Macmillan, J.B., and Chen, Z.J. (2009). RNA polymerase III detects cytosolic DNA and induces type I interferons through the RIG-I pathway. Cell *138*, 576-591.

Cui, S., Eisenacher, K., Kirchhofer, A., Brzozka, K., Lammens, A., Lammens, K., Fujita, T., Conzelmann, K.K., Krug, A., and Hopfner, K.P. (2008). The C-terminal regulatory domain is the RNA 5'-triphosphate sensor of RIG-I. Mol Cell *29*, 169-179.

Diebold, S.S., Kaisho, T., Hemmi, H., Akira, S., and Reis e Sousa, C. (2004). Innate antiviral responses by means of TLR7-mediated recognition of single-stranded RNA. Science *303*, 1529-1531.

Douglas, J., Cilliers, D., Coleman, K., Tatton-Brown, K., Barker, K., Bernhard, B., Burn, J., Huson, S., Josifova, D., Lacombe, D., *et al.* (2007). Mutations in RNF135, a gene within the NF1 microdeletion region, cause phenotypic abnormalities including overgrowth. Nat Genet *39*, 963-965.

Gack, M.U., Albrecht, R.A., Urano, T., Inn, K.S., Huang, I.C., Carnero, E., Farzan, M., Inoue, S., Jung, J.U., and Garcia-Sastre, A. (2009). Influenza A virus NS1 targets the ubiquitin ligase TRIM25 to evade recognition by the host viral RNA sensor RIG-I. Cell Host Microbe *5*, 439-449.

Gack, M.U., Kirchhofer, A., Shin, Y.C., Inn, K.S., Liang, C., Cui, S., Myong, S., Ha, T., Hopfner, K.P., and Jung, J.U. (2008). Roles of RIG-I N-terminal tandem CARD and splice variant in TRIM25-mediated antiviral signal transduction. Proc Natl Acad Sci U S A *105*, 16743-16748.

Gack, M.U., Shin, Y.C., Joo, C.H., Urano, T., Liang, C., Sun, L., Takeuchi, O., Akira, S., Chen, Z., Inoue, S., and Jung, J.U. (2007). TRIM25 RING-finger E3 ubiquitin ligase is essential for RIG-I-mediated antiviral activity. Nature *446*, 916-920.

Gao, D., Yang, Y.K., Wang, R.P., Zhou, X., Diao, F.C., Li, M.D., Zhai, Z.H., Jiang, Z.F., and Chen, D.Y. (2009). REUL is a novel E3 ubiquitin ligase and stimulator of retinoic-acid-inducible gene-I. PLoS One *4*, e5760.

Honda, K., Takaoka, A., and Taniguchi, T. (2006). Type I interferon [corrected] gene induction by the interferon regulatory factor family of transcription factors. Immunity *25*, 349-360.

Honda, K., Yanai, H., Takaoka, A., and Taniguchi, T. (2005). Regulation of the type I IFN induction: a current view. Int Immunol *17*, 1367-1378.

Horner, S.M., and Gale, M., Jr. (2009). Intracellular innate immune cascades and interferon defenses that control hepatitis C virus. J Interferon Cytokine Res *29*, 489-498.

Hornung, V., Ellegast, J., Kim, S., Brzozka, K., Jung, A., Kato, H., Poeck, H., Akira, S., Conzelmann, K.K., Schlee, M., *et al.* (2006). 5'-Triphosphate RNA is the ligand for RIG-I. Science *314*, 994-997.

Ishii, K.J., Coban, C., Kato, H., Takahashi, K., Torii, Y., Takeshita, F., Ludwig, H., Sutter, G., Suzuki, K., Hemmi, H., *et al.* (2006). A Toll-like receptor-independent antiviral response induced by double-stranded B-form DNA. Nat Immunol *7*, 40-48.

Ishii, K.J., Kawagoe, T., Koyama, S., Matsui, K., Kumar, H., Kawai, T., Uematsu, S., Takeuchi, O., Takeshita, F., Coban, C., and Akira, S. (2008). TANK-binding kinase-1 delineates innate and adaptive immune responses to DNA vaccines. Nature *451*, 725-729.

Ishikawa, H., and Barber, G.N. (2008). STING is an endoplasmic reticulum adaptor that facilitates innate immune signalling. Nature *455*, 674-678.

Ishikawa, H., Ma, Z., and Barber, G.N. (2009). STING regulates intracellular DNA-mediated, type I interferon-dependent innate immunity. Nature *461*, 788-792.

Kato, H., Sato, S., Yoneyama, M., Yamamoto, M., Uematsu, S., Matsui, K., Tsujimura, T., Takeda, K., Fujita, T., Takeuchi, O., and Akira, S. (2005). Cell type-specific involvement of RIG-I in antiviral response. Immunity *23*, 19-28.

Kato, H., Takeuchi, O., Sato, S., Yoneyama, M., Yamamoto, M., Matsui, K., Uematsu, S., Jung, A., Kawai, T., Ishii, K.J., *et al.* (2006). Differential roles of MDA5 and RIG-I helicases in the recognition of RNA viruses. Nature *441*, 101-105.

Kawai, T., Takahashi, K., Sato, S., Coban, C., Kumar, H., Kato, H., Ishii, K.J., Takeuchi, O., and Akira, S. (2005). IPS-1, an adaptor triggering RIG-I- and Mda5-mediated type I interferon induction. Nat Immunol *6*, 981-988.

Kumagai, Y., Takeuchi, O., Kato, H., Kumar, H., Matsui, K., Morii, E., Aozasa, K., Kawai, T., and Akira, S. (2007). Alveolar macrophages are the primary interferon-alpha producer in pulmonary infection with RNA viruses. Immunity *27*, 240-252.

Kumar, H., Kawai, T., Kato, H., Sato, S., Takahashi, K., Coban, C., Yamamoto, M., Uematsu, S., Ishii, K.J., Takeuchi, O., and Akira, S. (2006). Essential role of IPS-1 in innate immune responses against RNA viruses. J Exp Med *203*, 1795-1803.

Meylan, E., Curran, J., Hofmann, K., Moradpour, D., Binder, M., Bartenschlager, R., and Tschopp, J. (2005). Cardif is an adaptor protein in the RIG-I antiviral pathway and is targeted by hepatitis C virus. Nature *437*, 1167-1172.

Miranda, C., Roccato, E., Raho, G., Pagliardini, S., Pierotti, M.A., and Greco, A. (2006). The TFG protein, involved in oncogenic rearrangements, interacts with TANK and NEMO, two proteins involved in the NF-kappaB pathway. J Cell Physiol *208*, 154-160.

Nakhaei, P., Genin, P., Civas, A., and Hiscott, J. (2009). RIG-I-like receptors: sensing and responding to RNA virus infection. Semin Immunol *21*, 215-222.

Onoguchi, K., Yoneyama, M., Takemura, A., Akira, S., Taniguchi, T., Namiki, H., and Fujita, T. (2007). Viral infections activate types I and III interferon genes through a common mechanism. J Biol Chem *282*, 7576-7581.

Oshiumi, H., Matsumoto, M., Hatakeyama, S., and Seya, T. (2009). Riplet/RNF135, a RING finger protein, ubiquitinates RIG-I to promote interferon-beta induction during the early phase of viral infection. J Biol Chem *284*, 807-817.

Pichlmair, A., Schulz, O., Tan, C.P., Naslund, T.I., Liljestrom, P., Weber, F., and Reis e Sousa, C. (2006). RIG-I-mediated antiviral responses to single-stranded RNA bearing 5'-phosphates. Science *314*, 997-1001.

Rehwinkel, J., Tan, C.P., Goubau, D., Schulz, O., Pichlmair, A., Bier, K., Robb, N., Vreede, F., Barclay, W., Fodor, E., and Reis e Sousa, C. (2010). RIG-I detects viral genomic RNA during negative-strand RNA virus infection. Cell *140*, 397-408.

Saito, T., Hirai, R., Loo, Y.M., Owen, D., Johnson, C.L., Sinha, S.C., Akira, S., Fujita, T., and Gale, M., Jr. (2007). Regulation of innate antiviral defenses through a shared repressor domain in RIG-I and LGP2. Proc Natl Acad Sci U S A *104*, 582-587.

Saito, T., Owen, D.M., Jiang, F., Marcotrigiano, J., and Gale, M., Jr. (2008). Innate immunity induced by composition-dependent RIG-I recognition of hepatitis C virus RNA. Nature *454*, 523-527.

Seth, R.B., Sun, L., Ea, C.K., and Chen, Z.J. (2005). Identification and characterization of MAVS, a mitochondrial antiviral signaling protein that activates NF-kappaB and IRF 3. Cell *122*, 669-682.

Shigemoto, T., Kageyama, M., Hirai, R., Zheng, J., Yoneyama, M., and Fujita, T. (2009). Identification of loss of function mutations in human genes encoding RIG-I and MDA5: implications for resistance to type I diabetes. J Biol Chem *284*, 13348-13354.

Sun, Q., Sun, L., Liu, H.H., Chen, X., Seth, R.B., Forman, J., and Chen, Z.J. (2006). The specific and essential role of MAVS in antiviral innate immune responses. Immunity *24*, 633-642.

Suzuki, H., Fukunishi, Y., Kagawa, I., Saito, R., Oda, H., Endo, T., Kondo, S., Bono, H., Okazaki, Y., and Hayashizaki, Y. (2001). Protein-protein interaction panel using mouse full-length cDNAs. Genome Res *11*, 1758-1765.

Takahasi, K., Yoneyama, M., Nishihori, T., Hirai, R., Kumeta, H., Narita, R., Gale, M., Jr., Inagaki, F., and Fujita, T. (2008). Nonself RNA-sensing mechanism of RIG-I helicase and activation of antiviral immune responses. Mol Cell *29*, 428-440.

Takeuchi, O., and Akira, S. (2010). Pattern recognition receptors and inflammation. Cell

140, 805-820.

Xu, L.G., Wang, Y.Y., Han, K.J., Li, L.Y., Zhai, Z., and Shu, H.B. (2005). VISA is an adapter protein required for virus-triggered IFN-beta signaling. Mol Cell *19*, 727-740.

Yoneyama, M., and Fujita, T. (2009). RNA recognition and signal transduction by RIG-I-like receptors. Immunol Rev *227*, 54-65.

Yoneyama, M., and Fujita, T. (2010). Recognition of viral nucleic acids in innate immunity. Rev Med Virol *20*, 4-22.

Yoneyama, M., Kikuchi, M., Natsukawa, T., Shinobu, N., Imaizumi, T., Miyagishi, M., Taira, K., Akira, S., and Fujita, T. (2004). The RNA helicase RIG-I has an essential function in double-stranded RNA-induced innate antiviral responses. Nat Immunol *5*, 730-737.

Zeng, W., Sun, L., Jiang, X., Chen, X., Hou, F., Adhikari, A., Xu, M., and Chen, Z.J. (2010). Reconstitution of the RIG-I pathway reveals a signaling role of unanchored polyubiquitin chains in innate immunity. Cell *141*, 315-330.

Supplementary Figure Legends

Figure S1 (A) Structure of the mouse Riplet gene, targeting vector, and disrupted gene. Closed boxes indicate the coding exon of Riplet, and hatched boxes indicate Neo or TK gene coding region. The numbers in parentheses indicate the reading frame. If alternative splicing occurs to skip Ex2 and Ex3, the mRNA does not encode the C-terminal region of Riplet because reading frames of Ex1 and Ex4 are different from each other. Arrows indicate PCR primers used to detect short or long arm.

(B) PCR of mouse tail. Genomic DNA was extracted from wild-type and Riplet mice tails, and PCR was performed with primers shown in (A).

Figure S2

Splenocytes or GM-CSF-induced cDC from Riplet −/− or wild-type mice were analyzed by FACS using anti-mouse CD4, CD8, CD11b, CD11c, and/or PDCA1.

Figure S3

(A) HCV 3' UTR ss- and dsRNA were synthesized in vitro by T7 and/or SP6 RNA polymerase. RNA was treated with DNase I to remove template DNA and purified with TRIZOL reagent (Invitrogen). Wild-type and Riplet −/− MEFs were transfected in 24-well plates with 100 ng of HCV 3' UTR ss- or dsRNA and lipofectamine 2000 reagent. Nine hours after transfection, total RNA was extracted, and RT-qPCR was performed.

(B) Wild-type or Riplet −/− MEFs were infected with VSV at MOI = 5 for the

indicated time periods. Total RNA was extracted from the cells, and RT-qPCR were performed with primers designed to detect the expression of IFN-λ, which amplify both IFN- λ 2 and λ 3. Expression of β-actin was used to normalize each samples.

Figure S4

(A, B) Wild-type and Riplet −/− MEFs were infected with VSV at MOI = 0.2 (A) or 1 (B). Total RNA was extracted at the indicated time periods, and RT-qPCR was performed. Expression of β-actin was used to normalize each sample. (C) Wild-type or Riplet −/− MEFs were transfected with or without 0.8 μg of HCV 3' UTR dsRNA. Nine hours after transfection, total RNA was extracted and RT-qPCR was performed. Expression of β-actin was used to normalize each sample. The most right bars indicate the expression of IFN-β during VSV infection.

Figure S5

(A, B) BM-DC form wild-type or Riplet −/− mice were stimulated with LPS, and amounts of IFN-β (A) and IL-6 (B) in culture supernatant were measured by ELISA.

Figure S6

(A, B) Wild-type or Riplet −/− mice were infected intranasally $2x10^6$ pfu of VSV. Amounts of IFN-α (A) and -β (B) in mouse serum 30 hours after infection were measured by ELISA.

Supplementary Table 1: Primer list

mRiplet Ex2 primer F:	GGTGACAGTACAGAAAAGTACC
mRiplet Ex2 primer R:	GTCCCTCTTGAACTTACCGTGG
Neo primer F:	TCAGCGCAGGGGCGCCCGGTTCTTT
Neo primer R:	ATCGACAAGACCGGCTTCCATCCG
mRiplet-F1:	CTGGACAGGACAATGCACAAGG
mRiplet-R1:	GACAAGTGAGAAGCTTTCCTGG
mIFN-a2-qF1:	TACTCAGCAGACCTTGAACC
mIFN-a2-qR1:	GGTACACAGTGATCCTGTGG
mCcl5 F:	TGCCCACGTCAAGGAGTATTT
mCcl5 R:	TCGAGTGACAAACACGACTGC
mIFNb For:	CCAGCTCCAAGAAAGGACGA
mIFNb Rev	CGCCCTGTAGGTGAGGTTGAT
mouseIP-10 F:	GTGTTGAGATCATTGCCACGA
mouseIP-10 R:	GCGTGGCTTCACTCCAGTTAA
mouse beta actin for:	TTTGCAGCTCCTTCGTTGC
mouse beta actin rev:	TCGTCATCCATGGCGAACT
mIPS-1 F:	AGCCCTCCAGAGAGCATCAA
mIPS-1 R:	GAGGCAACATTTGCTGCGT
mMDA5 F:	GCTGCCCAGAAGACAACACAG
mMDA5 R:	CGACAGCAGGCAGAAGACACT
mRIG-I F:	GCCCTGTACCATGCAGGTTAC

mRIG-I R:	AGTCCCAACTTTCGATGGCTT
mTICAM-1 F:	TGTTGGAAAGCAGTGGCCTAT
mTICAM-1 R:	GATGACGTGGTGTTCTGCAGA
mTLR3 F:	TTGCGTTGCGAAGTGAAGAA
mTLR3 R:	ACTTGCCAATTGTCTGGAAACA
mTRIM25 F:	CGACCTGGAGTACAAACTGAGG
mTRIM25 R:	ACTTGCGCAAGGAGCTGGTCTC

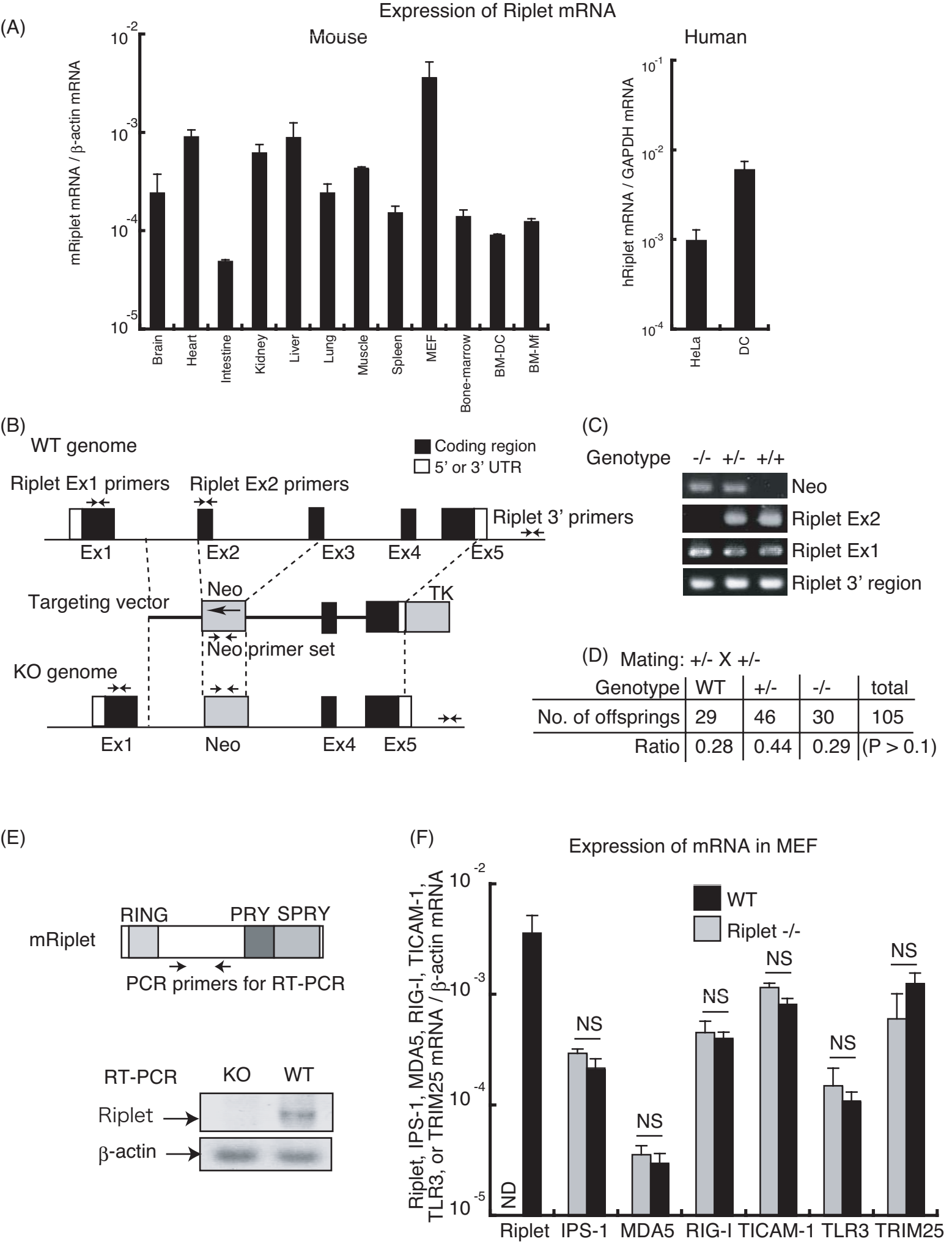

Genotype	WT	+/-	-/-	total
No. of offsprings	29	46	30	105
Ratio	0.28	0.44	0.29	(P > 0.1)

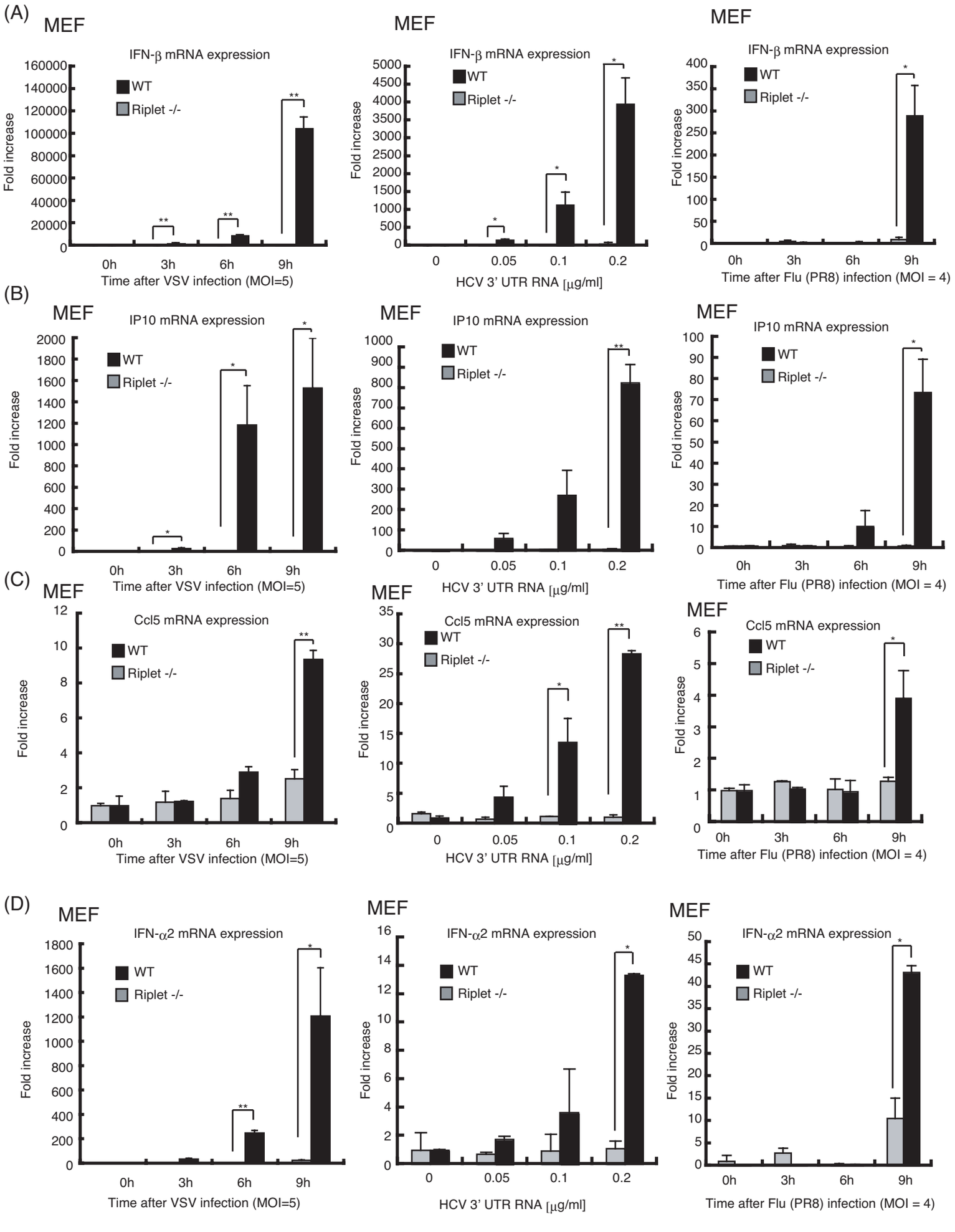
(A)
MEF
IFN-β mRNA expression
WT
Riplet -/-
Fold increase
Time after VSV infection (MOI=5)
HCV 3' UTR RNA [μg/ml]
Time after Flu (PR8) infection (MOI = 4)
(B)
IP10 mRNA expression
(C)
Ccl5 mRNA expression
(D)
IFN-α2 mRNA expression
0h
3h
6h
9h
0
0.05
0.1
0.2

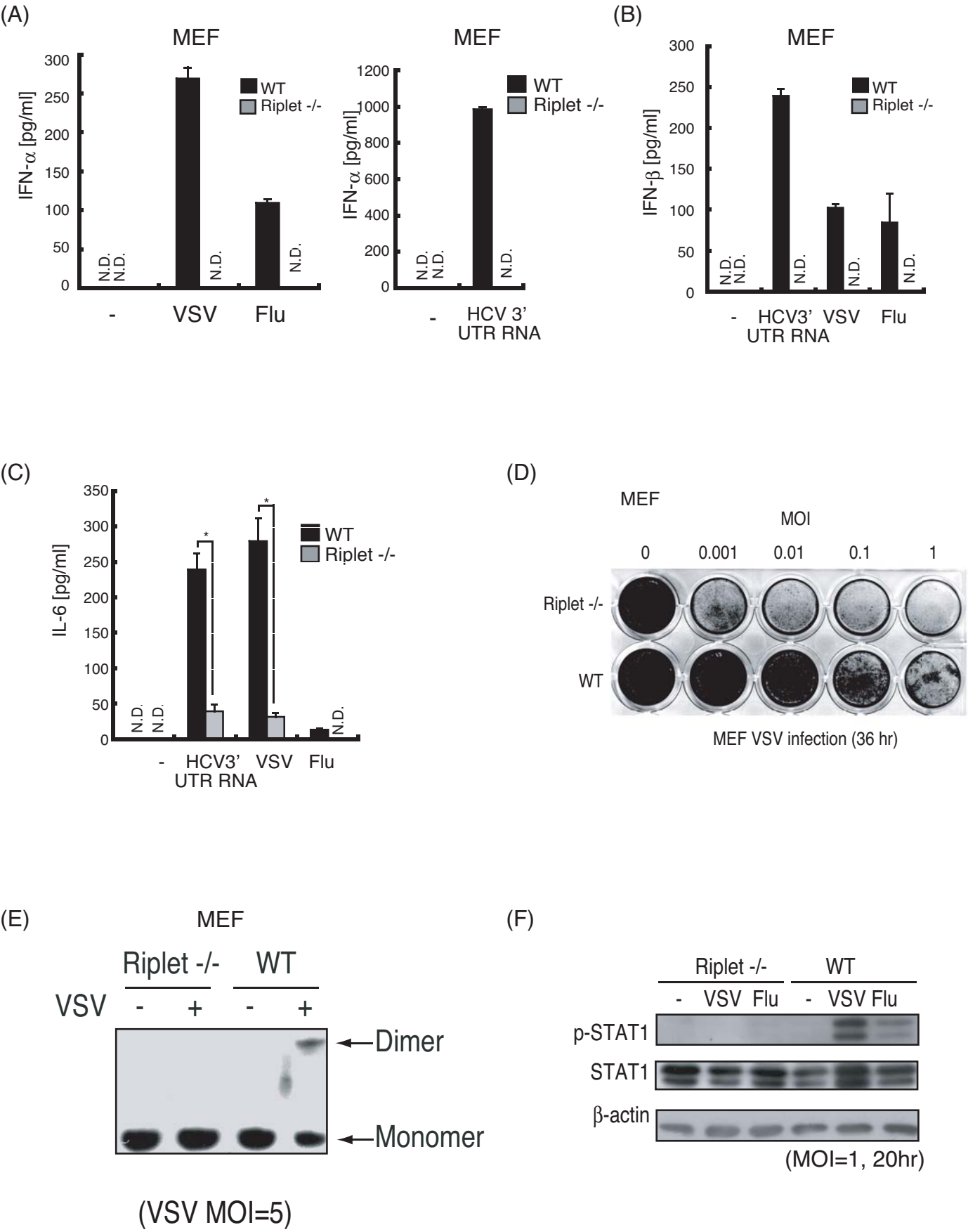
(A)
MEF
IFN-α [pg/ml]
300
250
200
150
100
50
0
WT
Riplet -/-
N.D.
N.D.
N.D.
N.D.
-
VSV
Flu
MEF
IFN-α [pg/ml]
1200
1000
800
600
400
200
0
WT
Riplet -/-
N.D.
N.D.
N.D.
-
HCV 3'
UTR RNA
(B)
MEF
IFN-β [pg/ml]
300
250
200
150
100
50
0
WT
Riplet -/-
N.D.
N.D.
N.D.
N.D.
-
HCV3' UTR RNA
VSV
Flu
(C)
IL-6 [pg/ml]
350
300
250
200
150
100
50
0
WT
Riplet -/-
*
*
N.D.
N.D.
N.D.
-
HCV3' UTR RNA
VSV
Flu
(D)
MEF
MOI
0
0.001
0.01
0.1
1
Riplet -/-
WT
MEF VSV infection (36 hr)
(E)
MEF
Riplet -/-
WT
VSV
-
+
-
+
Dimer
Monomer
(VSV MOI=5)
(F)
Riplet -/-
WT
-
VSV
Flu
-
VSV
Flu
p-STAT1
STAT1
β-actin
(MOI=1, 20hr)

(A)

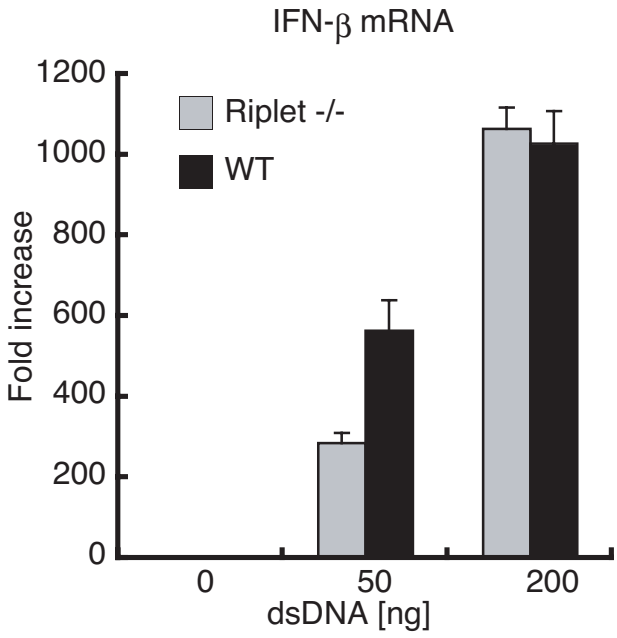
IFN-β mRNA
Riplet -/-
WT
Fold increase
1200
1000
800
600
400
200
0
0
50
200
dsDNA [ng]

(B)

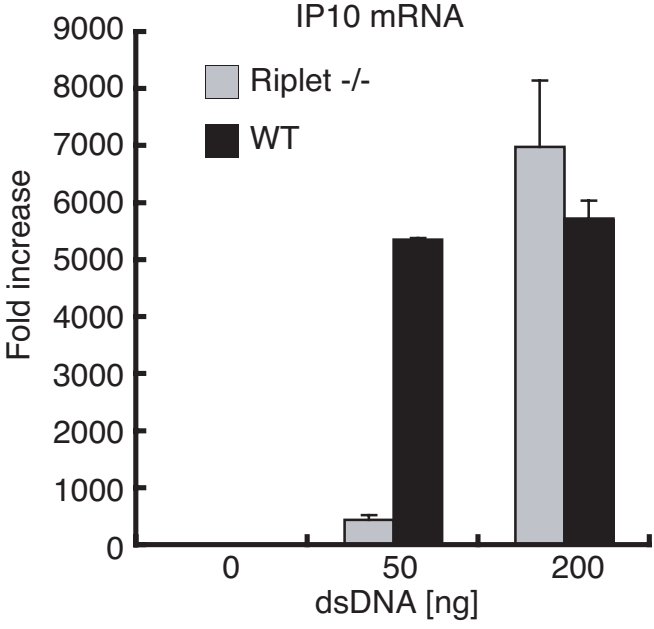
IP10 mRNA
Riplet -/-
WT
Fold increase
9000
8000
7000
6000
5000
4000
3000
2000
1000
0
0
50
200
dsDNA [ng]

(C)

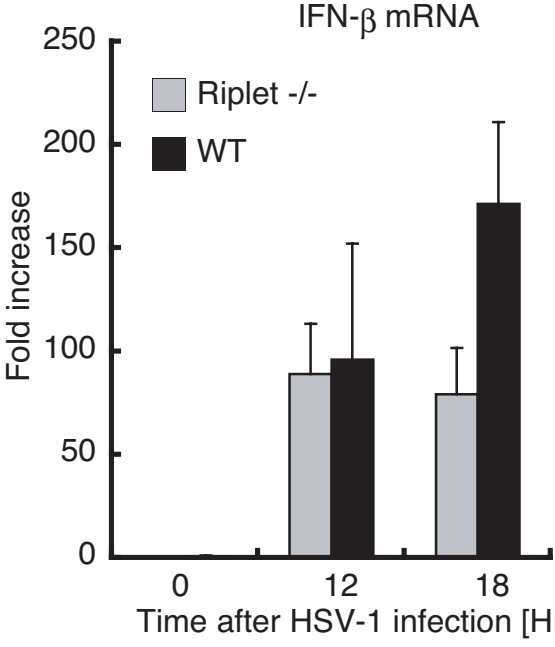
IFN-β mRNA
Riplet -/-
WT
Fold increase
250
200
150
100
50
0
0
12
18
Time after HSV-1 infection [Hr]

Figure 5

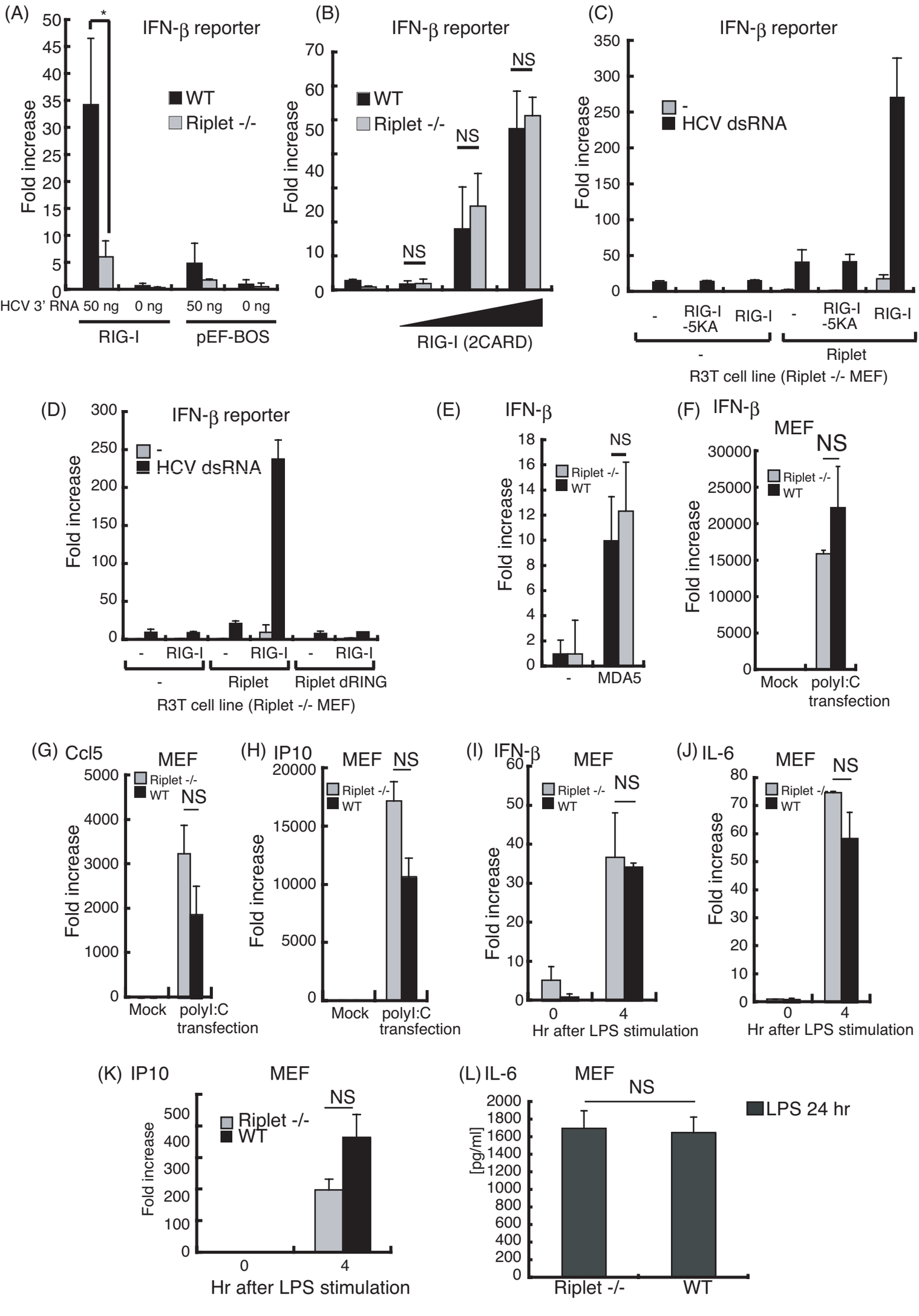
(A)
IFN-β reporter
Fold increase
WT
Riplet -/-
*
HCV 3' RNA 50 ng 0 ng 50 ng 0 ng
RIG-I
pEF-BOS
(B)
IFN-β reporter
Fold increase
WT
Riplet -/-
NS
NS
NS
RIG-I (2CARD)
(C)
IFN-β reporter
Fold increase
-
HCV dsRNA
- RIG-I -5KA RIG-I - RIG-I -5KA RIG-I
-
Riplet
R3T cell line (Riplet -/- MEF)
(D)
IFN-β reporter
Fold increase
-
HCV dsRNA
- RIG-I - RIG-I - RIG-I
-
Riplet
Riplet dRING
R3T cell line (Riplet -/- MEF)
(E)
IFN-β
Fold increase
Riplet -/-
WT
NS
-
MDA5
(F)
IFN-β
MEF
Fold increase
Riplet -/-
WT
NS
Mock
polyI:C transfection
(G)
Ccl5
MEF
Fold increase
Riplet -/-
WT
NS
Mock
polyI:C transfection
(H)
IP10
MEF
NS
Fold increase
Riplet -/-
WT
Mock
polyI:C transfection
(I)
IFN-β
MEF
Fold increase
Riplet -/-
WT
NS
0
4
Hr after LPS stimulation
(J)
IL-6
MEF
NS
Fold increase
Riplet -/-
WT
0
4
Hr after LPS stimulation
(K)
IP10
MEF
NS
Fold increase
Riplet -/-
WT
0
4
Hr after LPS stimulation
(L)
IL-6
MEF
NS
[pg/ml]
LPS 24 hr
Riplet -/-
WT

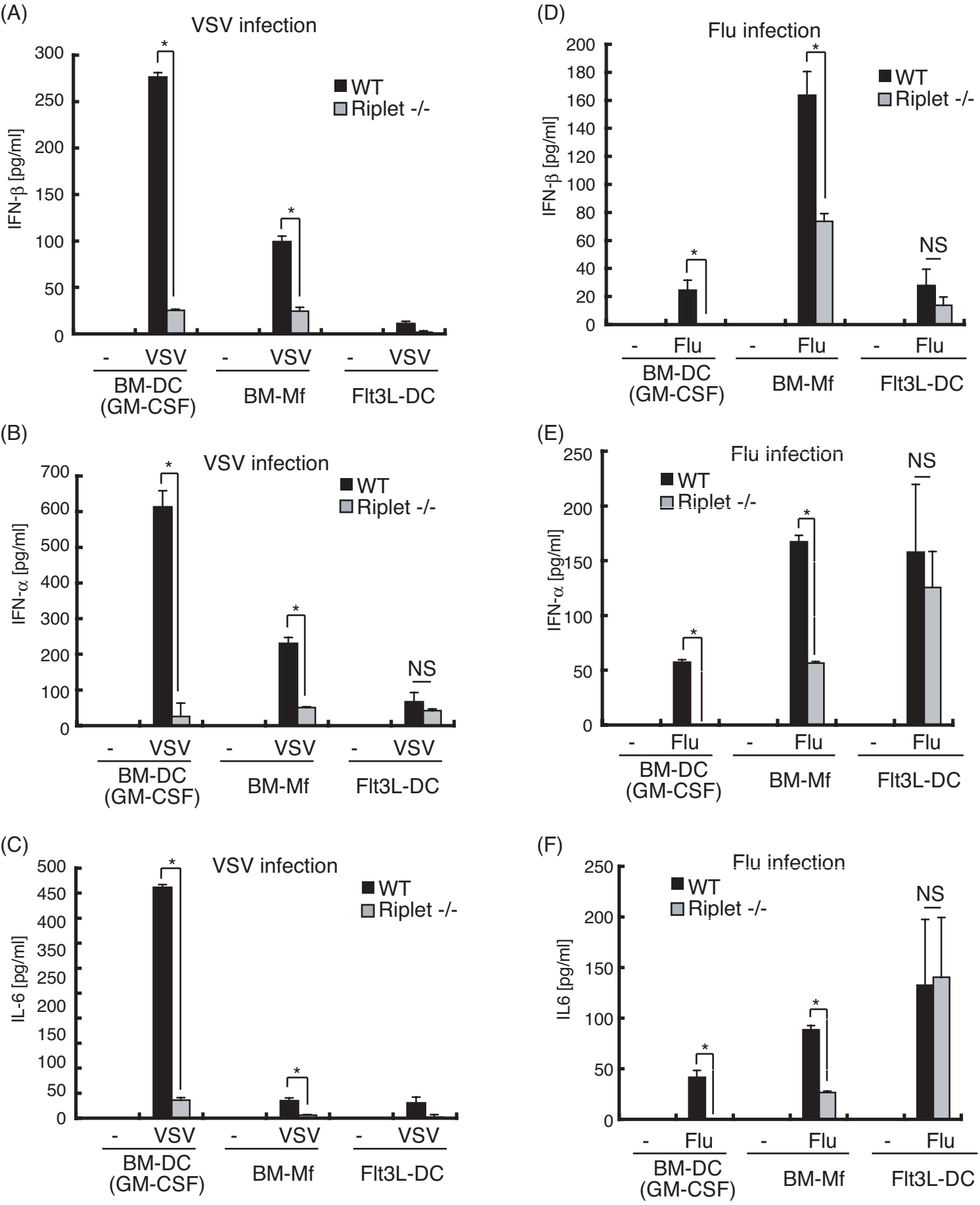
(A)
VSV infection
IFN-β [pg/ml]
300
250
200
150
100
50
0
WT
Riplet -/-
*
*
- VSV
BM-DC (GM-CSF)
- VSV
BM-Mf
- VSV
Flt3L-DC
(B)
VSV infection
IFN-α [pg/ml]
700
600
500
400
300
200
100
0
WT
Riplet -/-
*
*
NS
- VSV
BM-DC (GM-CSF)
- VSV
BM-Mf
- VSV
Flt3L-DC
(C)
VSV infection
IL-6 [pg/ml]
500
450
400
350
300
250
200
150
100
50
0
WT
Riplet -/-
*
*
- VSV
BM-DC (GM-CSF)
- VSV
BM-Mf
- VSV
Flt3L-DC
(D)
Flu infection
IFN-β [pg/ml]
200
180
160
140
120
100
80
60
40
20
0
WT
Riplet -/-
*
*
NS
- Flu
BM-DC (GM-CSF)
- Flu
BM-Mf
- Flu
Flt3L-DC
(E)
Flu infection
IFN-α [pg/ml]
250
200
150
100
50
0
WT
Riplet -/-
*
*
NS
- Flu
BM-DC (GM-CSF)
- Flu
BM-Mf
- Flu
Flt3L-DC
(F)
Flu infection
IL6 [pg/ml]
250
200
150
100
50
0
WT
Riplet -/-
*
*
NS
- Flu
BM-DC (GM-CSF)
- Flu
BM-Mf
- Flu
Flt3L-DC

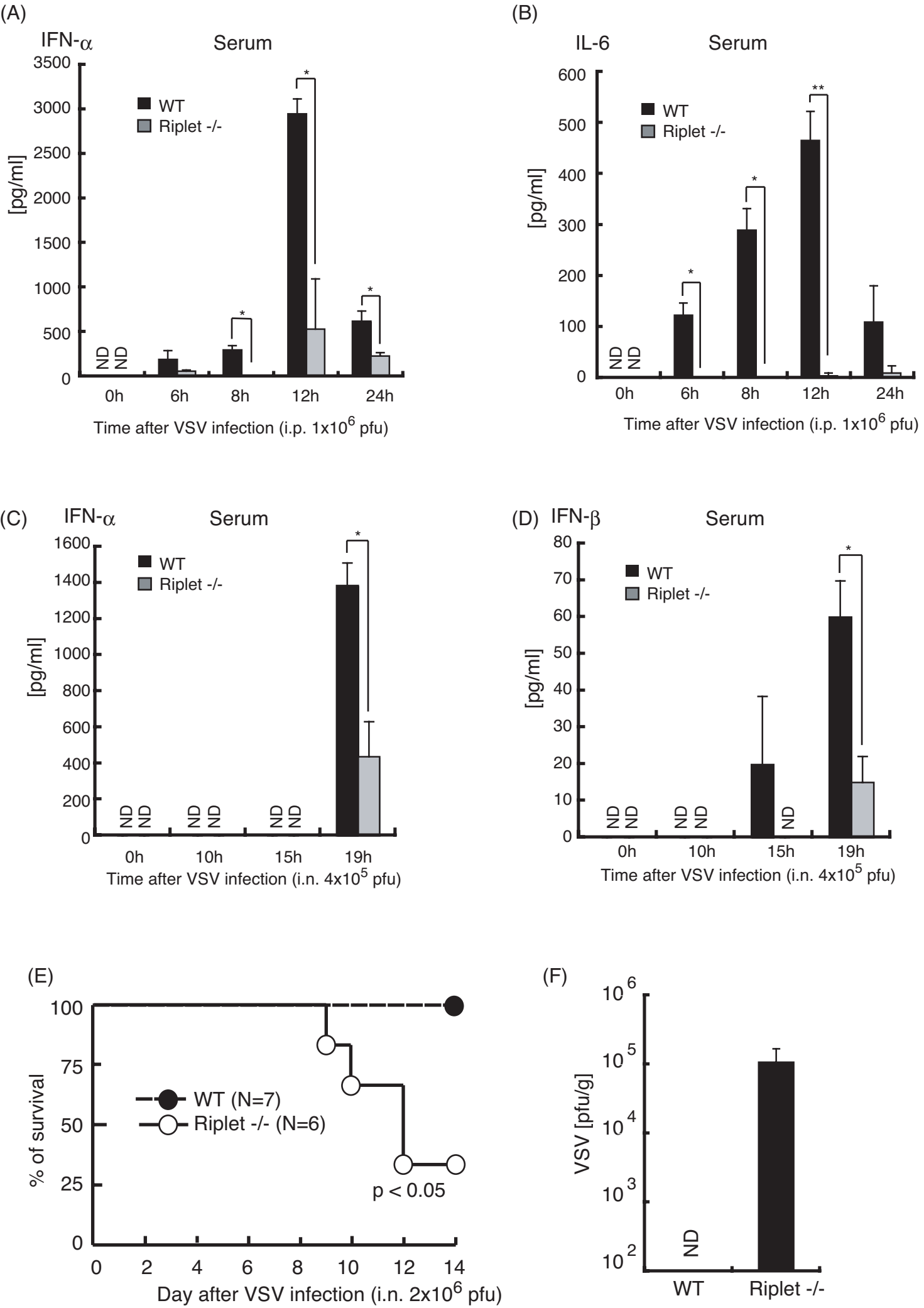
(A)
IFN-α
Serum
WT
Riplet -/-
[pg/ml]
3500
3000
2500
2000
1500
1000
500
0
ND ND
0h
6h
8h
12h
24h
Time after VSV infection (i.p. 1x10^6 pfu)
(B)
IL-6
Serum
WT
Riplet -/-
[pg/ml]
600
500
400
300
200
100
0
ND ND
0h
6h
8h
12h
24h
Time after VSV infection (i.p. 1x10^6 pfu)
(C)
IFN-α
Serum
WT
Riplet -/-
[pg/ml]
1600
1400
1200
1000
800
600
400
200
0
ND ND
ND ND
ND ND
0h
10h
15h
19h
Time after VSV infection (i.n. 4x10^5 pfu)
(D)
IFN-β
Serum
WT
Riplet -/-
[pg/ml]
80
70
60
50
40
30
20
10
0
ND ND
ND ND
ND
0h
10h
15h
19h
Time after VSV infection (i.n. 4x10^5 pfu)
(E)
% of survival
100
75
50
25
0
WT (N=7)
Riplet -/- (N=6)
p < 0.05
0
2
4
6
8
10
12
14
Day after VSV infection (i.n. 2x10^6 pfu)
(F)
VSV [pfu/g]
10^6
10^5
10^4
10^3
10^2
ND
WT
Riplet -/-

(A)

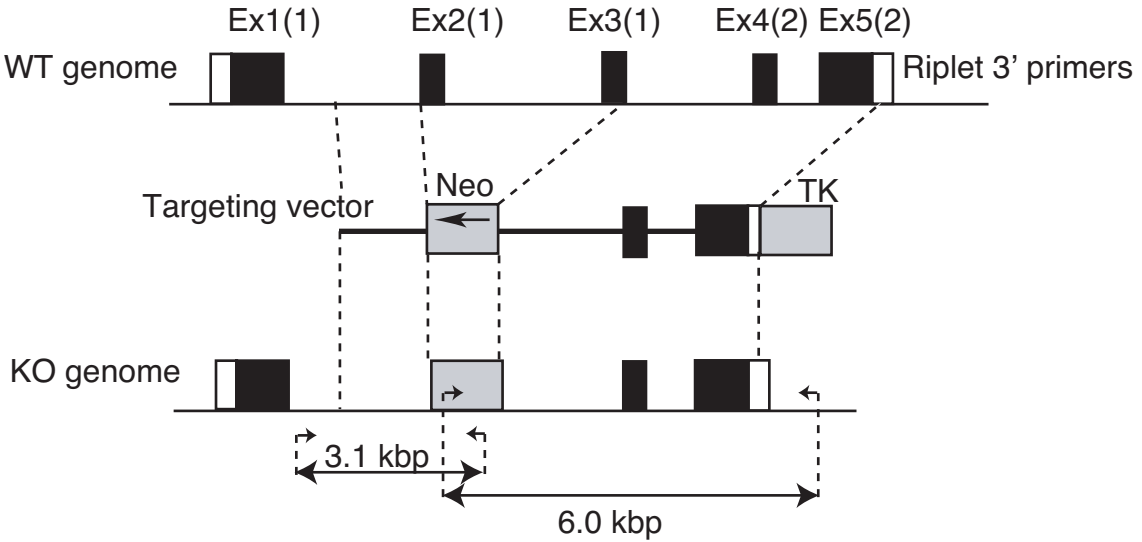
Ex1(1)
Ex2(1)
Ex3(1)
Ex4(2) Ex5(2)
WT genome
Riplet 3' primers
Targeting vector
Neo
TK
KO genome
3.1 kbp
6.0 kbp

(B)

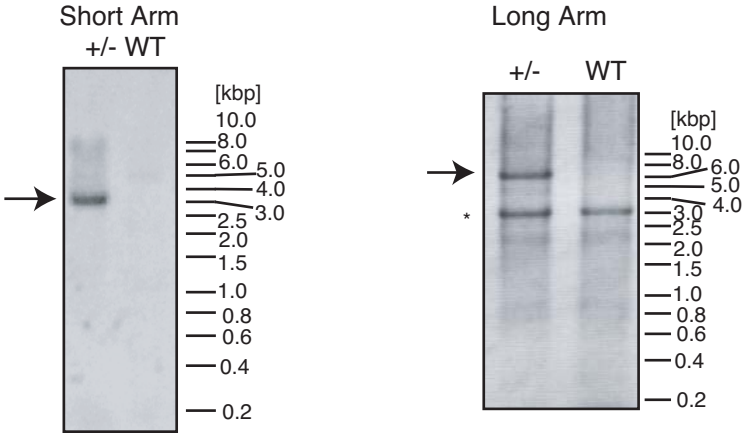
Short Arm
+/- WT
[kbp]
10.0
8.0
6.0
5.0
4.0
3.0
2.5
2.0
1.5
1.0
0.8
0.6
0.4
0.2
Long Arm
+/-
WT
*
[kbp]
10.0
8.0
6.0
5.0
4.0
3.0
2.5
2.0
1.5
1.0
0.8
0.6
0.4
0.2

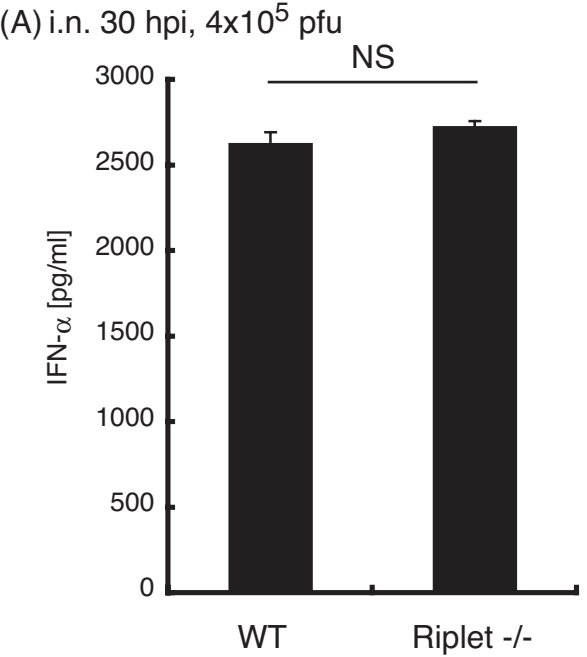
(A) i.n. 30 hpi, 4x10^5 pfu
NS
3000
2500
2000
1500
1000
500
0
IFN-α [pg/ml]
WT
Riplet -/-

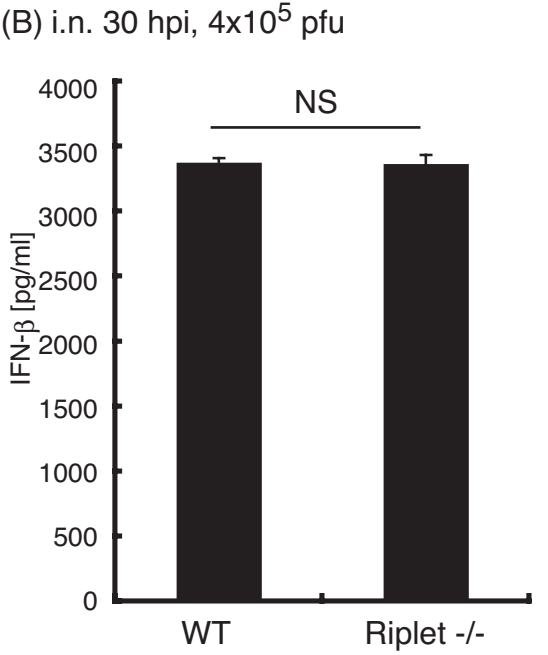
(B) i.n. 30 hpi, 4x10^5 pfu
NS
4000
3500
3000
2500
2000
1500
1000
500
0
IFN-β [pg/ml]
WT
Riplet -/-

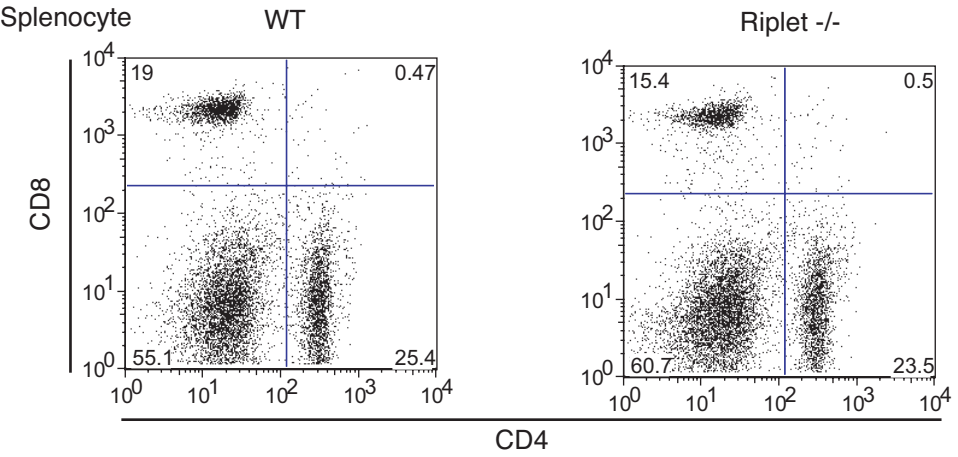
Splenocyte
WT
Riplet -/-
CD8
CD4
19
0.47
55.1
25.4
15.4
0.5
60.7
23.5

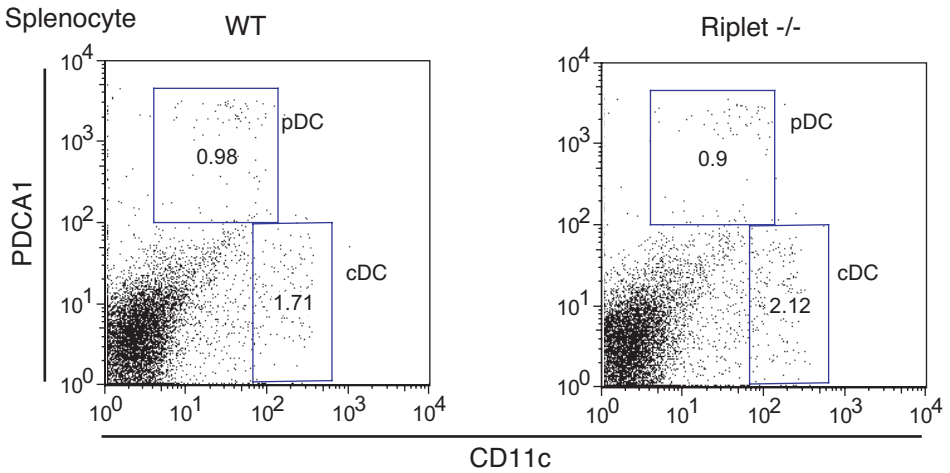
Splenocyte
WT
Riplet -/-
PDCA1
CD11c
pDC
cDC
0.98
1.71
0.9
2.12

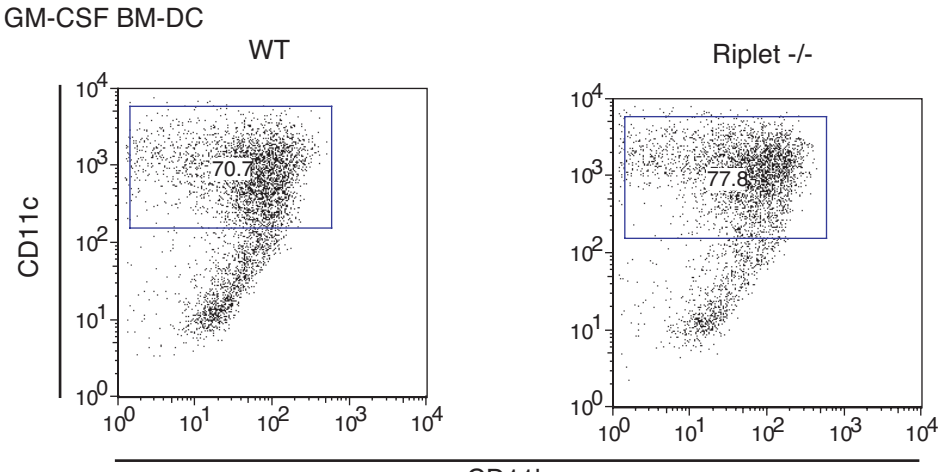
GM-CSF BM-DC
WT
Riplet -/-
CD11c
CD11b
70.7
77.8

(A)

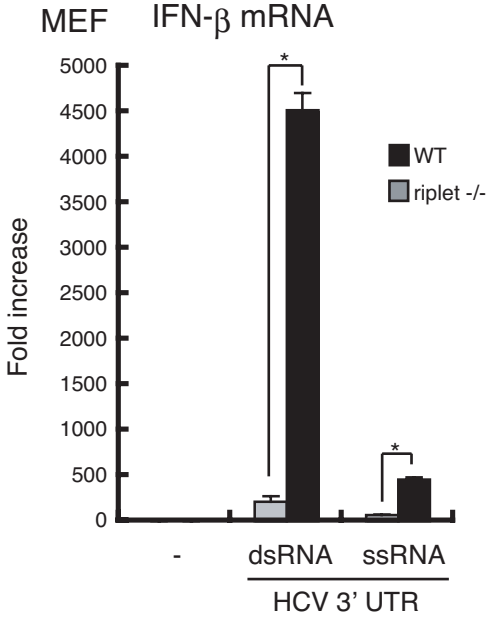
MEF IFN-β mRNA
Fold increase
5000
4500
4000
3500
3000
2500
2000
1500
1000
500
0
*
*
WT
riplet -/-
-
dsRNA
ssRNA
HCV 3' UTR

(B)

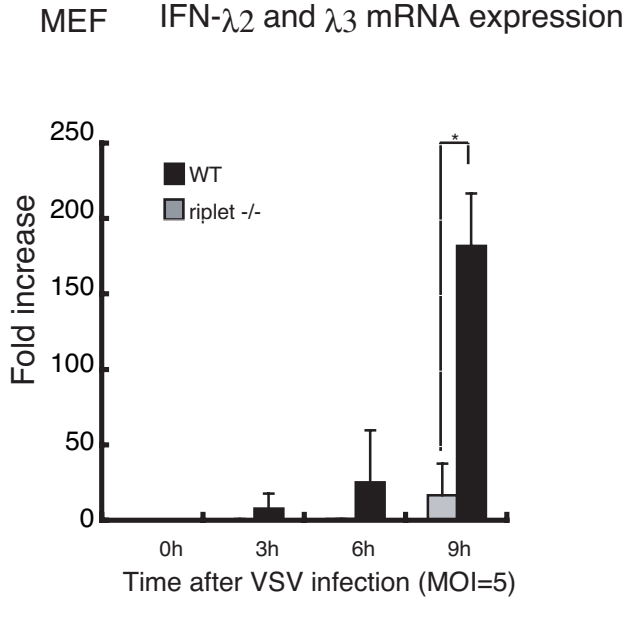
MEF IFN-λ2 and λ3 mRNA expression
Fold increase
250
200
150
100
50
0
*
WT
riplet -/-
0h
3h
6h
9h
Time after VSV infection (MOI=5)

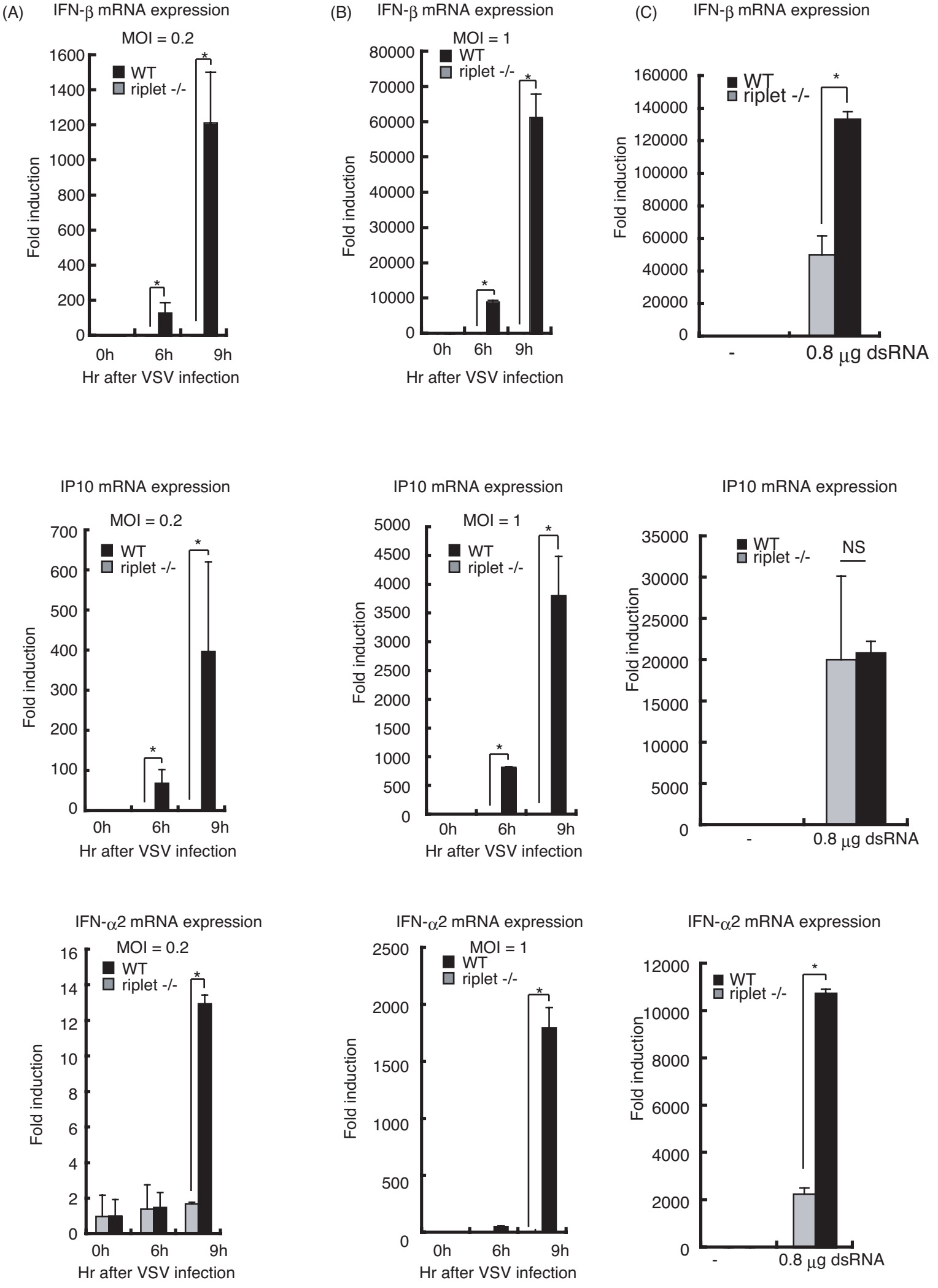
(A)
IFN-β mRNA expression
MOI = 0.2
WT
riplet -/-
Fold induction
0h
6h
9h
Hr after VSV infection
(B)
IFN-β mRNA expression
MOI = 1
WT
riplet -/-
Fold induction
0h
6h
9h
Hr after VSV infection
(C)
IFN-β mRNA expression
WT
riplet -/-
Fold induction
-
0.8 μg dsRNA
IP10 mRNA expression
MOI = 0.2
WT
riplet -/-
Fold induction
0h
6h
9h
Hr after VSV infection
IP10 mRNA expression
MOI = 1
WT
riplet -/-
Fold induction
0h
6h
9h
Hr after VSV infection
IP10 mRNA expression
WT
riplet -/-
NS
Fold induction
-
0.8 μg dsRNA
IFN-α2 mRNA expression
MOI = 0.2
WT
riplet -/-
Fold induction
0h
6h
9h
Hr after VSV infection
IFN-α2 mRNA expression
MOI = 1
WT
riplet -/-
Fold induction
0h
6h
9h
Hr after VSV infection
IFN-α2 mRNA expression
WT
riplet -/-
Fold induction
-
0.8 μg dsRNA

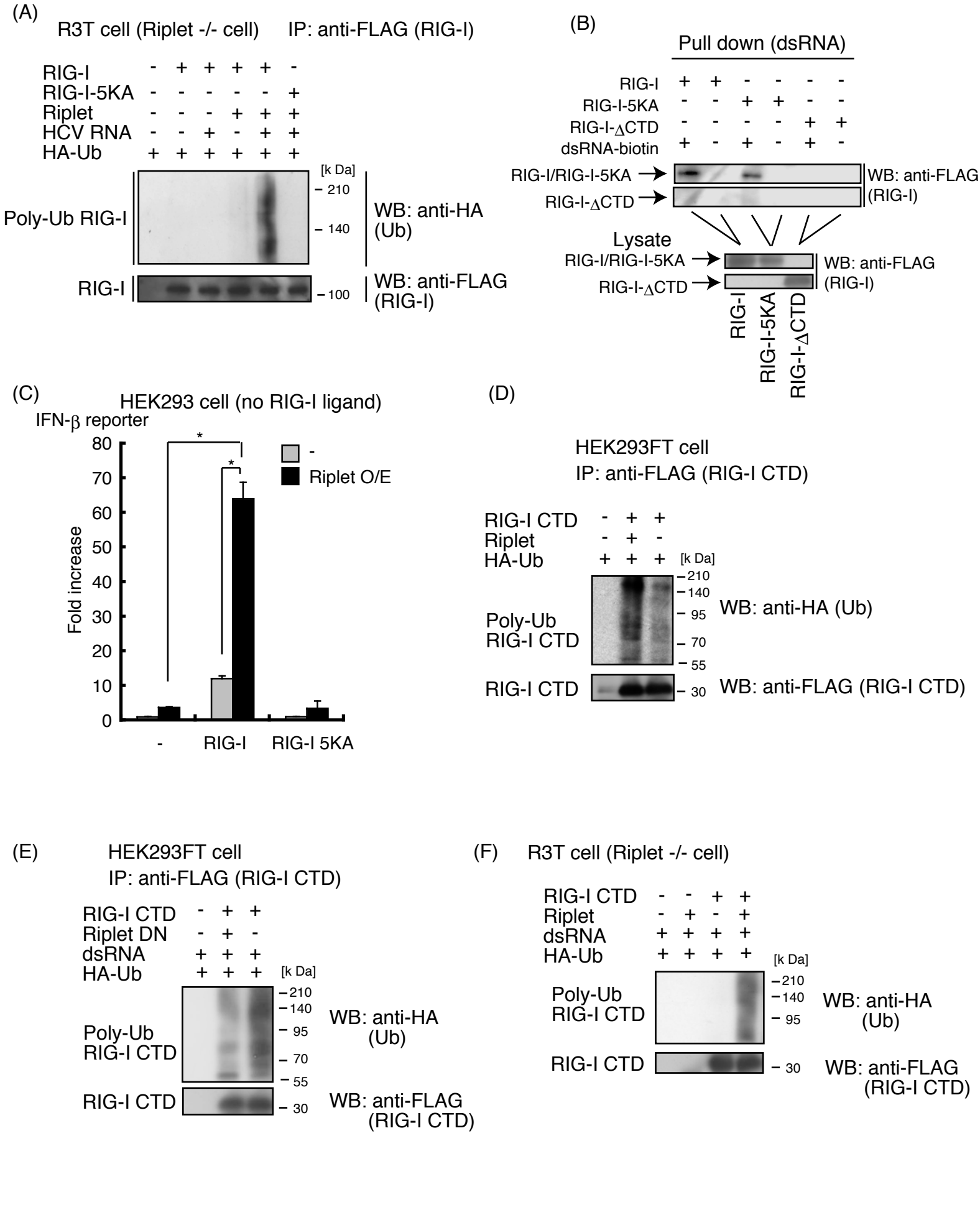
(A)
R3T cell (Riplet -/- cell)
IP: anti-FLAG (RIG-I)
RIG-I
RIG-I-5KA
Riplet
HCV RNA
HA-Ub
[k Da]
210
140
Poly-Ub RIG-I
WB: anti-HA (Ub)
RIG-I
100
WB: anti-FLAG (RIG-I)
(B)
Pull down (dsRNA)
RIG-I
RIG-I-5KA
RIG-I-ΔCTD
dsRNA-biotin
RIG-I/RIG-I-5KA
RIG-I-ΔCTD
WB: anti-FLAG (RIG-I)
Lysate
RIG-I/RIG-I-5KA
RIG-I-ΔCTD
WB: anti-FLAG (RIG-I)
RIG-I
RIG-I-5KA
RIG-I-ΔCTD
(C)
HEK293 cell (no RIG-I ligand)
IFN-β reporter
Fold increase
80
70
60
50
40
30
20
10
0
*
*
-
Riplet O/E
-
RIG-I
RIG-I 5KA
(D)
HEK293FT cell
IP: anti-FLAG (RIG-I CTD)
RIG-I CTD
Riplet
HA-Ub
[k Da]
210
140
95
70
55
Poly-Ub RIG-I CTD
WB: anti-HA (Ub)
RIG-I CTD
30
WB: anti-FLAG (RIG-I CTD)
(E)
HEK293FT cell
IP: anti-FLAG (RIG-I CTD)
RIG-I CTD
Riplet DN
dsRNA
HA-Ub
[k Da]
210
140
95
70
55
Poly-Ub RIG-I CTD
WB: anti-HA (Ub)
RIG-I CTD
30
WB: anti-FLAG (RIG-I CTD)
(F)
R3T cell (Riplet -/- cell)
RIG-I CTD
Riplet
dsRNA
HA-Ub
[k Da]
210
140
95
Poly-Ub RIG-I CTD
WB: anti-HA (Ub)
RIG-I CTD
30
WB: anti-FLAG (RIG-I CTD)

Figure S6

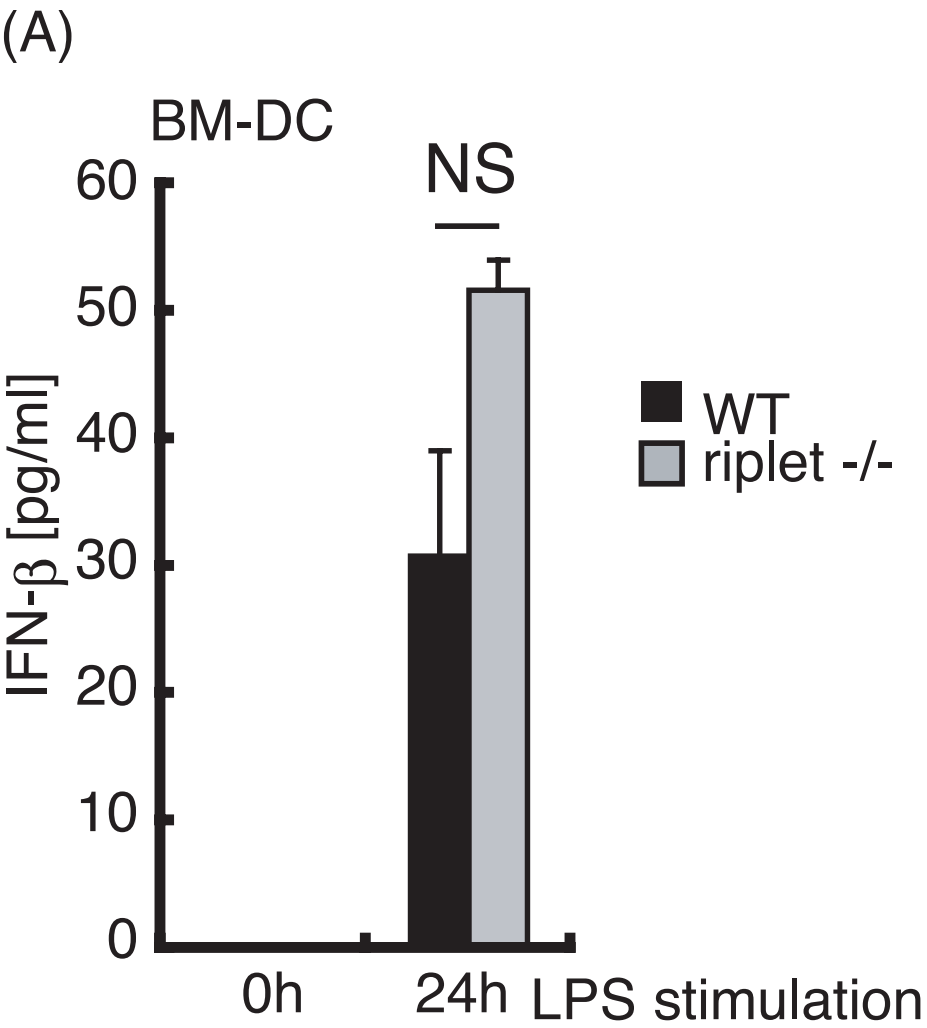
(A)
BM-DC
NS
60
50
40
30
20
10
0
IFN-β [pg/ml]
WT
riplet -/-
0h
24h
LPS stimulation

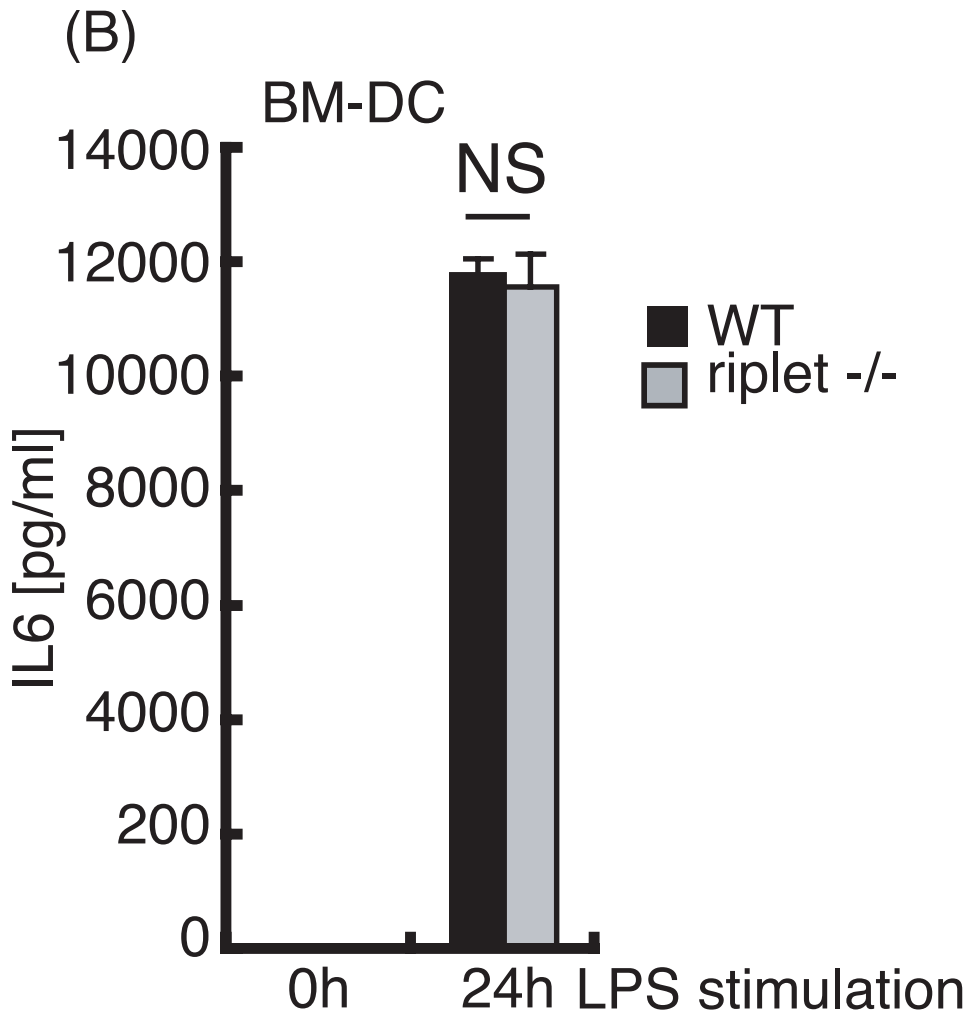
(B)
BM-DC
NS
14000
12000
10000
8000
6000
4000
200
0
IL6 [pg/ml]
WT
riplet -/-
0h
24h
LPS stimulation

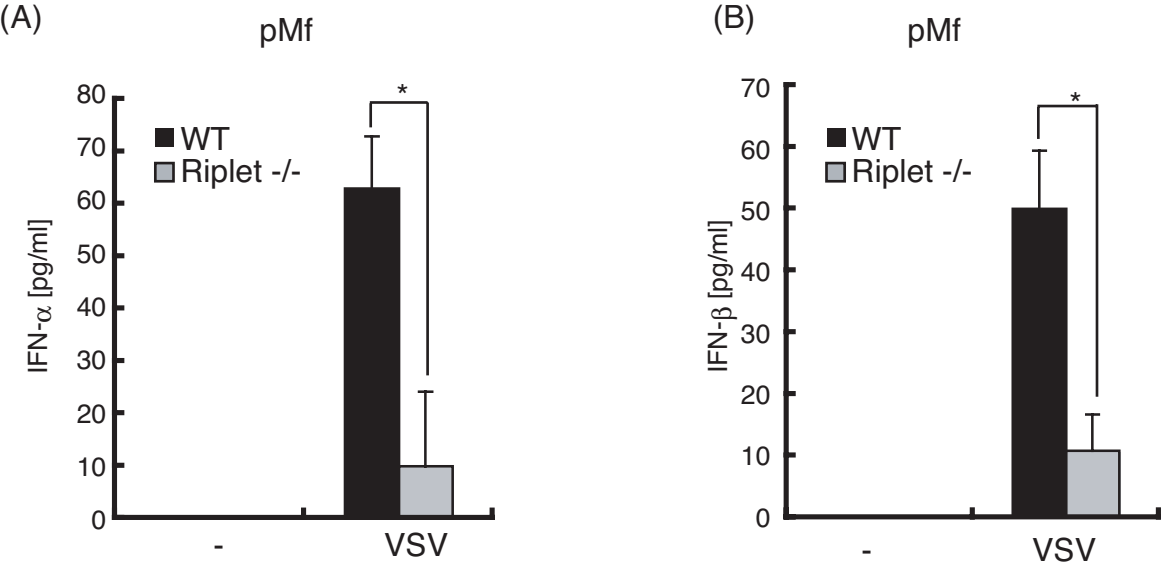
(A)
pMf
80
70
60
50
40
30
20
10
0
IFN-α [pg/ml]
WT
Riplet -/-
*
-
VSV
(B)
pMf
70
60
50
40
30
20
10
0
IFN-β [pg/ml]
WT
Riplet -/-
*
-
VSV

Figure S8

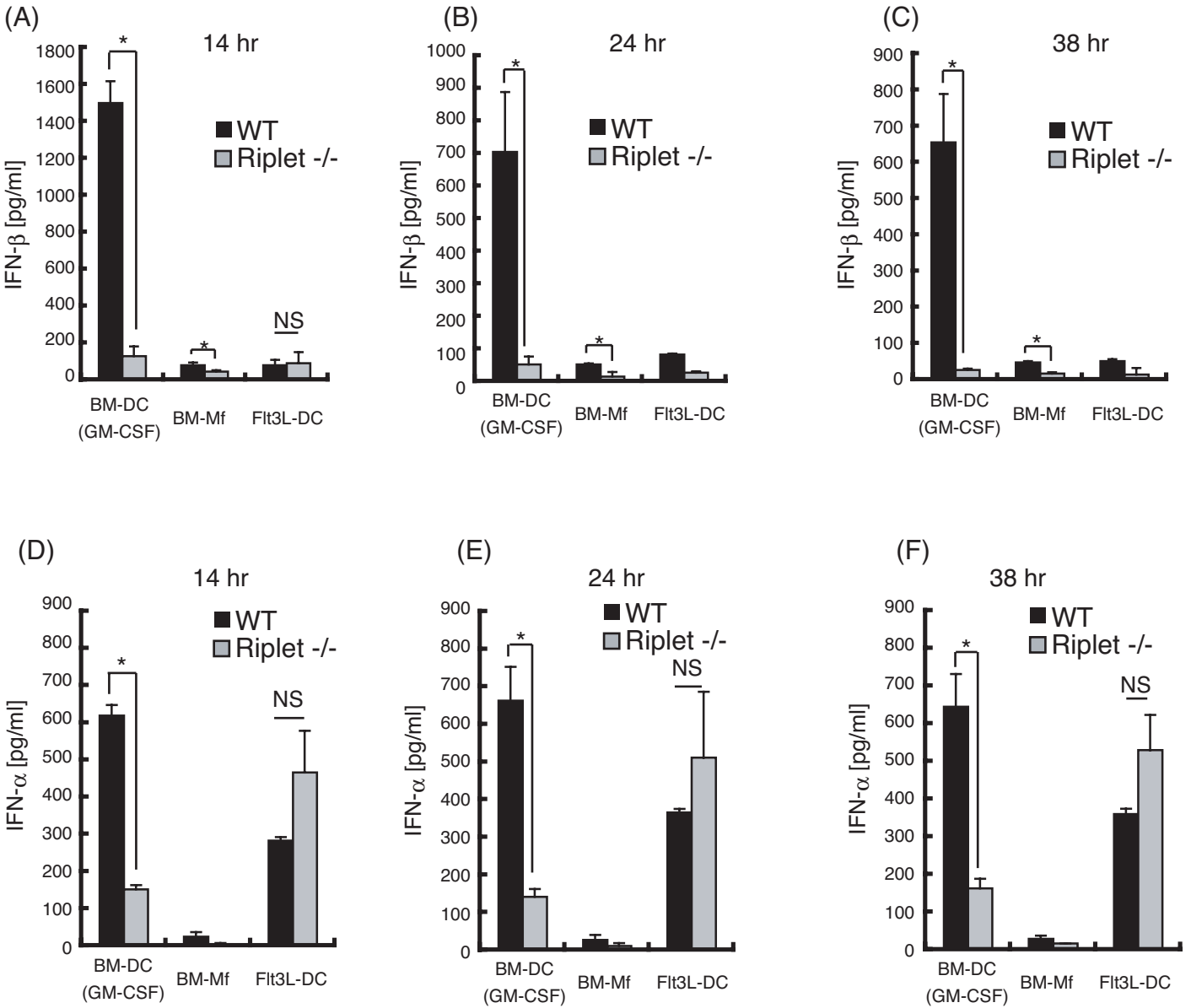
(A)
14 hr
IFN-β [pg/ml]
1800
1600
1400
1200
1000
800
600
400
200
0
WT
Riplet -/-
*
*
NS
BM-DC (GM-CSF)
BM-Mf
Flt3L-DC
(B)
24 hr
IFN-β [pg/ml]
1000
900
800
700
600
500
400
300
200
100
0
WT
Riplet -/-
*
*
BM-DC (GM-CSF)
BM-Mf
Flt3L-DC
(C)
38 hr
IFN-β [pg/ml]
900
800
700
600
500
400
300
200
100
0
WT
Riplet -/-
*
*
BM-DC (GM-CSF)
BM-Mf
Flt3L-DC
(D)
14 hr
IFN-α [pg/ml]
900
800
700
600
500
400
300
200
100
0
WT
Riplet -/-
*
NS
BM-DC (GM-CSF)
BM-Mf
Flt3L-DC
(E)
24 hr
IFN-α [pg/ml]
900
800
700
600
500
400
300
200
100
0
WT
Riplet -/-
*
NS
BM-DC (GM-CSF)
BM-Mf
Flt3L-DC
(F)
38 hr
IFN-α [pg/ml]
900
800
700
600
500
400
300
200
100
0
WT
Riplet -/-
*
NS
BM-DC (GM-CSF)
BM-Mf
Flt3L-DC

Figure S9

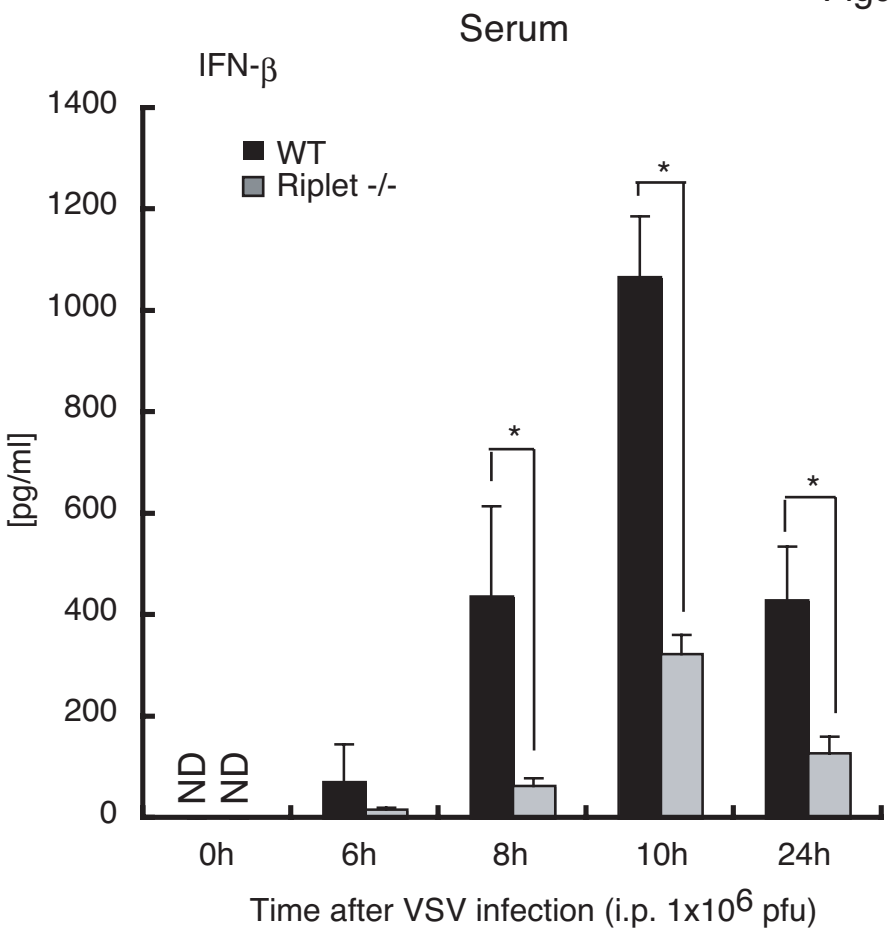
Serum
IFN-β
1400
1200
1000
800
600
400
200
0
[pg/ml]
WT
Riplet -/-
ND
ND
*
*
*
0h
6h
8h
10h
24h
Time after VSV infection (i.p. 1x10^6 pfu)